



Time and temperature dependency of carbon dioxide triggered metal(loid) mobilization in soil



Judith Mehlhorn ^a, James M. Byrne ^b, Andreas Kappler ^b, Britta Planer-Friedrich ^{a,*}

^a University of Bayreuth, Environmental Geochemistry, Bayreuth Center for Ecology and Environmental Research (BayCEER), Universitaetsstrasse 30, D-95440 Bayreuth, Germany

^b University of Tuebingen, Geomicrobiology, Center for Applied Geosciences, Sigwartstrasse 10, D-72076 Tuebingen, Germany

ARTICLE INFO

Article history:

Received 21 June 2016

Received in revised form

13 September 2016

Accepted 16 September 2016

Available online 17 September 2016

Keywords:

Mofette

Fluvisol

Carbon Capture and Storage (CCS)

Microbial iron reduction

Czech Republic

ABSTRACT

Assessing the influence of CO₂ on soil and aquifer geochemistry is a task of increasing interest when considering risk assessment for geologic carbon sequestration. Leakage and CO₂ ascent can lead to soil acidification and mobilization of potentially toxic metals and metalloids due to desorption or dissolution reactions. We studied the CO₂ influence on an Fe(III) (oxyhydr)oxide rich, gleyic Fluvisol sampled in close vicinity to a Czech mofette site and compared the short-term CO₂ influence in laboratory experiments with observations on long-term influence at the natural site. Six week batch experiments with/without CO₂ gas flow at 3 different temperatures and monitoring of liquid phase metal(loid) concentrations revealed two main short-term mobilization processes. Within 1 h to 1 d after CO₂ addition, mobilization of weakly adsorbed metal cations occurred due to surface protonation, most pronounced for Mn (2.5–3.3 fold concentration increase, mobilization rates up to $278 \pm 18 \mu\text{g Mn kg}_{\text{soil}}^{-1} \text{d}^{-1}$) and strongest at low temperatures. However, total metal(loid) mobilization by abiotic desorption was low. After 1–3 d significant Fe mobilization due to microbially-triggered Fe(III) (oxyhydr)oxide dissolution began and continued throughout the experiment (up to 111 ± 24 fold increase or up to $1.9 \pm 0.6 \text{ mg Fe kg}_{\text{soil}}^{-1} \text{d}^{-1}$). Rates increased at higher temperature and with a higher content of organic matter. The Fe(III) mineral dissolution was coupled to co-release of incorporated metal(loid)s, shown for As (up to 16 ± 7 fold, $11 \pm 8 \mu\text{g As kg}_{\text{soil}}^{-1} \text{d}^{-1}$). At high organic matter content, re-immobilization due to resorption reactions could be observed for Cu. The already low pH (4.5–5.0) did not change significantly during Fe(III) reduction due to buffering from sorption and dissolution reactions, but a drop in redox potential (from > +500 mV to minimum $+340 \pm 20$ mV) occurred due to oxygen depletion. We conclude that microbial processes following CO₂ induction into a soil can contribute significantly to metal(loid) mobilization, especially at optimal microbial growth conditions (moderate temperature, high organic carbon content) and should be considered for carbon sequestration monitoring and risk assessment.

© 2016 Elsevier Ltd. All rights reserved.

1. Introduction

The storage of carbon dioxide (CO₂) in geological structures (geologic carbon storage, GCS) is a promising option for the reduction of industrial greenhouse gas emissions and currently tested and practiced in numerous projects all over the world. Even though GCS sites are carefully selected in order to guarantee safe storage over centuries, leakage of CO₂ can never be completely ruled out and risks for overlying aquifers and soils have to be assessed (IPCC, 2005; Jun et al., 2012, 2013).

* Corresponding author.

E-mail address: b.planer-friedrich@uni-bayreuth.de (B. Planer-Friedrich).

One possibility to study long-term influence of CO₂ on soils and aquifers is using natural analogues (Lewicki et al., 2007; Pearce, 2006; Schütze et al., 2012). Cold, volcanic CO₂ exhalation sites, called mofettes, can have CO₂ partial pressures ($p(\text{CO}_2)$) of up to 1 (Bräuer et al., 2004; Kämpf et al., 2007) and thus represent excellent sites to study effects on soil and pore water conditions. Dissolution of CO₂ in pore water and dissociation of carbonic acid causes soil acidification and can lead to mobilization of trace elements due to mineral dissolution reactions (Blume and Felix-Henningsen, 2009; Kharaka et al., 2006, 2010; Mehlhorn et al., 2014; Wang and Jaffe, 2004; Zheng et al., 2009, 2012). The influence of high CO₂ partial pressures on iron (Fe) oxides and oxyhydroxides (hereafter summarized as Fe(III) (oxyhydr)oxides) was studied in

detail for a Czech grassland mofette site in Rennert et al. (2011, 2012). They found that Fe minerals in the mofette were of weak crystallinity and extractable pedogenic Fe(III) (oxyhydr)oxide content showed a negative correlation with $p(\text{CO}_2)$. Solid Fe phases were dominated by Fe(III) incorporated in silicates and fine grained Fe(II) as well as mixed Fe(II)/Fe(III) mineral phases, while pedogenic Fe(III) (oxyhydr)oxides could only be detected along old root channels. They concluded that Fe release by weathering of parent material is decreased in the mofettes and the small amount of Fe(II) released from weathering is not re-oxidized to Fe(III) (oxyhydr)oxides due to the absence of oxygen.

The organic matter content in mofettes can be significantly increased compared to surrounding sites which are unaffected by CO_2 . This increase is attributed to decreased decomposition rates under anoxic conditions in mofettes (Flechsigt et al., 2008; Maček et al., 2009; Rennert et al., 2011; Videmšek et al., 2009) and an additional organic matter input from autotrophic microbial carbon fixation of geogenic CO_2 (Beulig et al., 2015; Nowak et al., 2015). Furthermore, a shift in microbial community towards anaerobic, acidophilic microorganisms, a lowered microbial diversity as well as the exclusion of meso- and macroscopic eukaryotes have been observed in mofettes, which contributes to organic matter accumulation (Beulig et al., 2016; Fernández-Montiel et al., 2016; Frerichs et al., 2013; Nowak et al., 2015; Oppermann et al., 2010; Šibanc et al., 2014). Solid organic matter quality analyzed by ^{13}C NMR did not seem to be affected by geogenic CO_2 in a mofette with moderate $p(\text{CO}_2)$ (Rennert and Pfanz, 2015) while Fourier-transform infrared spectroscopy on a transect with $p(\text{CO}_2)$ up to 1 revealed detectable changes in organic matter quality with increased lignin concentrations at higher $p(\text{CO}_2)$ (Rennert et al., 2011).

Investigations on natural soil and pore water samples from a Czech mofette site conducted by our working group in 2013 confirmed the negative correlation of total Fe content in soil and $p(\text{CO}_2)$ as well as the increased organic matter content in mofettes compared to an adjacent CO_2 unaffected reference soil (Mehlhorn et al., 2014). We also showed that the reduced content of Fe(III) (oxyhydr)oxides led to an increased mobility of arsenic (As) in the mofettes while other elements, especially copper (Cu), showed a decreased net-mobility due to adsorption to organic matter in the mofettes.

However, as useful as natural analogues are for assessing the long-term effects of CO_2 on soil and aquifers, they cannot provide any information on time dependencies of the observed (im)mobilization processes. Also, other influences on metal(loid) mobilization, like microbial activity or seasonal effects can hardly be studied in a quantitative way at natural sites, since the current state of most mofettes represents the effects of CO_2 influence over decades or centuries. To further assess the pathway that leads to conditions found in mofettes, laboratory batch experiments with controlled CO_2 gas purging can help to increase the current knowledge by distinguishing between different (im)mobilization pathways and be used to determine mobilization rates. Numerous batch studies on the influence of CO_2 on different sediment materials exist indicating that mobilization reactions due to desorption or mineral dissolution are the dominating short-term processes following a CO_2 intrusion into an aquifer (e.g. Kirsch et al., 2014; Lawter et al., 2016; Little and Jackson, 2010; Smyth et al., 2009). However, also re-adsorption or formation of secondary minerals can occur and lead to net-immobilization of certain metal(loid)s (e.g. Lawter et al., 2015; Lu et al., 2010; Mickler et al., 2013; Shao et al., 2015). Significant knowledge gaps still exist on the influence of other relevant geochemical factors, like redox condition, microbial activity, or mineral composition (Harvey et al., 2012). The microbial influence in particular is not yet completely understood since the effects of

microbial activity on metal(loid) mobility largely depend on the community present in the sediment or soil, which will differ significantly between different sites. Microbes can either enhance mobilization rates by altering existing equilibria and triggering the dissolution of certain minerals, e.g., the dissolution of Fe(III) (oxyhydr)oxides (Kirk et al., 2013), or promote mineral precipitation by increasing alkalinity or direct biological carbonate formation (Harvey et al., 2016; Kirk et al., 2013; Lions et al., 2014 and references therein).

To further investigate the short-term effects of CO_2 intrusion on metal(loid) mobility, we conducted batch experiments with hitherto CO_2 unaffected soil suspensions from a gleyic Fluvisol in close vicinity to mofettes already studied in Mehlhorn et al. (2014). The aim of this study was (i) to distinguish between different mobilization and immobilization processes by detailed monitoring of metal(loid) concentrations during CO_2 incubation, (ii) to get qualitative information about the microbial influence on the (im) mobilization reactions by variation of incubation temperature, and (iii) to determine mobilization rates for certain metal(loid)s under the conditions prevailing in mofettes, hence, helping to increase our understanding of the risks arising from potential GCS leakage into soil and aquifers. Based on the results gained from our study at the natural mofette site, we hypothesized that mobilization of metal cations due to desorption will be the dominating short-term effect, combined with low total liquid phase concentration increases. Further, we expected mobilization of Fe and other metal(loid)s due to the reductive dissolution of Fe(III) (oxyhydr)oxides, a potentially microbially-triggered process that should be accelerated by increased incubation temperatures. The main advantage of using soil material from close vicinity of mofettes for the batch experiments is the possibility of direct comparison between experimental results on short-term CO_2 influence with results from field studies on long-term effects.

2. Material and methods

2.1. Site description and sampling

Soil and water samples for batch experiments were collected in a mofette area in northwestern Czech Republic. The mofettes are located in the flood plain of the river Plesná, which follows the north-south striking Počátky-Plesná Zone where CO_2 -rich mantle gasses ascend from a magma chamber in the lower earth crust (Bankwitz et al., 2003). We selected a mofette, already studied in Mehlhorn et al. (2014), that is located in direct vicinity of the river Plesná and thus is water saturated all year. Soil samples were not taken directly from the mofette, but from a "reference site" some meters away which was selected based on vegetation changes (N 50°08'43.7" E 12°27'1.4", for a more detailed description see Mehlhorn et al. (2014)). Thus, the soil selected for batch experiments is similar to the mofette soils but not CO_2 influenced. The first sampling took place on March 2nd, 2015. The vegetation and root zone were removed before 1 kg of soil, previously classified as gleyic Fluvisol (Beulig et al., 2016), was taken from a depth between 20 and 30 cm and packed in airtight closed plastic bags. The selected sampling depth was chosen based on results from 2013, where the most pronounced metal(loid) concentration differences between mofette and reference soils were found at approximately 25 cm depth. For the batch experiments, we chose river water as groundwater analogue, since groundwater was not available in the amounts needed. Metal(loid) concentrations in the river water were similar to or lower than in natural pore water (see Section 3.1) which justified the usage of river water as analogue for an uncontaminated aquifer. Two liters of river water were sampled as close as possible to the soil sampling site (distance approx. 15 m), a few

cm below the surface in 1 L-polypropylene bottles without gaseous headspace. The samples were kept cool during transport to the laboratory, where the river water was filtered (0.2 μm , cellulose-acetate filter, CHROMAFIL[®] Xtra) to remove particles and microorganisms. Before storage at 8 °C, the head space of the water bottles was filled with nitrogen and sealed airtight. The soil bags were opened and closed again in an anoxic COY-glovebox (95% N₂, 5% H₂) in order to remove oxygen from the gas phase. Afterwards, the bags were sealed and stored at 8 °C.

The second sampling took place on August 21st, 2015, and was conducted analogous to the first sampling. Due to the relatively hot and dry summer (average temperature of 19.5 °C in August 2015 and 231 mm precipitation between May and August 2015, compared to a 1961–1990 average of 15.7 °C and 272 mm precipitation in the same time span for the Karlovy Vary region, CHMI (2015)) the soil was exceptionally dry and had a relatively high root content. We therefore took the soil from a depth of 30–40 cm, where there were less roots and the humidity was slightly higher. Sample preparation in the laboratory was the same as for the first sampling.

2.2. Batch experiments

We conducted two batch experiments, one with temperature variation and one with variation of initial soil conditions. The first experiment (Batch Experiment I) started 1 d after the first sampling and lasted 42 d. Three different temperatures were applied to the batches in order to lower (16 °C) or stimulate (35 °C) microbial activity compared to room temperature (22 °C) and imitate different seasons. While 16 and 22 °C are typical average soil temperatures for spring, summer, and fall season in Central Europe (PIK, 2016), the relatively warm 35 °C were chosen to simulate maximum microbial activity when soil is exposed to direct sunlight on a warm summer day. Each differently treated set consisted of 7 batch reactors: a triplicate of batches with soil and water phase that were not treated with CO₂ (controls), a triplicate of batches with soil and water phase that were treated with CO₂ gas flow (treatments), and one batch that contained only water and was treated with CO₂ gas flow (water blank). The batches were prepared in 250 mL glass bottles, that were filled with 50 g of fresh soil and 75 mL of filtered river water (soil:water ratio 1:1.5) or with 75 mL of filtered river water only for the water blanks, and stoppered with a chlorobutyl septum each. Since the soil appeared to be relatively homogenous, there was no further treatment before the beginning of the experiment except for the removal of bigger roots and plant debris. The batches with CO₂ treatment were connected to the CO₂ gas flow (28 \pm 5 mL min⁻¹) with one long needle as gas inlet and one short needle as gas outlet. The batches without CO₂ treatment only received a short needle to guarantee gas exchange with the atmosphere. One set of samples was placed at room temperature ("RT" 22 \pm 1 °C), one set was placed in a thermoelectric cool box (MOBICOOL V26) for cooling ("C" 16 \pm 1 °C), and one set was placed in a heated water bath ("H" 35 \pm 0.1 °C). All batches were covered with aluminum foil to exclude light radiation. After 10 min of gas flow, all batches were shaken softly to mix liquid and solid phase. The mixing was repeated daily during the whole experiment. Gas flow was controlled daily with a bubble counter at the outlet needle and needles were exchanged in case of blockage. Sampling of the liquid phase of all batches was conducted 1 h, 1, 3, 7, 14, 28, and 42 d after the start of the experiment. The gas flow was turned off 10 min before sampling in order to let bigger particles settle from the liquid phase. Between 1.5 and 5 mL of the liquid phase were removed from the batch with needle and syringe and filtered (0.2 μm , cellulose-acetate filter, CHROMAFIL[®] Xtra). Redox potential and pH (WTW pH meter Multi340i equipped with a SenTix pH

electrode and a SenTix ORP redox electrode) were measured immediately after sampling to minimize oxygen influence, and 1.5 mL of the remaining sample were stabilized with 15 μL of 8 M HNO₃ to prevent precipitation and stored at 8 °C until determination of total Fe, Mn, As, and Cu concentrations by inductively coupled plasma mass spectrometry (ICP-MS). For the last time step (42 d), an additional 2 mL of sample was stabilized in N₂-purged septum vials and stored at 8 °C for analysis of dissolved CO₂ and CH₄ by gas chromatography (GC). Each batch was weighed before and after the experiment for calculation of evaporation loss. For analysis of the solid phase, the remaining supernatant was removed, samples were freeze-dried and ground into a powder. Soil pH was measured in 0.01 M CaCl₂ solution (w/v ratio 1:2.5, WTW pH meter Multi340i equipped with a SenTix pH electrode). Total Fe, As, Mn, and Cu concentrations were determined with ICP-MS, after microwave digestion (MARS Xpress, CEM) with 10 mL aqua regia per 100 mg soil sample (program: 20 min heating to 160 °C, 15 min holding, 20 min cooling) in filtered (0.2 μm , cellulose-acetate filter, CHROMAFIL[®] Xtra) and diluted extracts.

Since the heated batches ("H") showed the most interesting mobilization processes, this part of the experiment was repeated a second time (Batch Experiment II). This time, the initial soil conditions were varied in order to get more information on the influence of season and microbial activity on mobilization processes. For one set of batches ("H2"), the soil used was the same as for Batch Experiment I ("fresh spring soil"), but this time the soil had been stored under anoxic and dark conditions at 8 °C for 11 weeks ("stored spring soil"). This long storage increased the crystallinity of the Fe(III) (oxyhydr)oxides and thus should have made them less easily accessible for microorganisms (see Section 3.2). Experimental conditions and sampling were the same as in Batch Experiment I, except that no samples for dissolved CO₂ and CH₄ analysis were taken and that the experiment was finished after 41 d. For the other set of batches ("H3"), fresh soil and water samples were collected from the Czech site in August 2015, 4 d before starting the experiment ("fresh summer soil"). Due to the relatively hot summer and the high organic carbon content (especially fine root material that was hardly removable), the microbial activity was expected to be high compared to the other batches. Experimental setup and sampling were equal to H2. However, due to the extremely low soil moisture, this part of the experiment lasted only 28 d, since a big part of the added water was absorbed immediately by soil and less supernatant water for liquid sampling remained.

2.3. Quantification of microbial activity

We determined most probable numbers (MPN) for three samples of the stored spring soil from Batch Experiment II (one initial, one treatment, and one control sample) to quantify the amount of cultivatable heterotrophic aerobic, Fe(III)-reducing, and sulfate-reducing microorganisms. A detailed description of MPN methods and results can be found in the Supplementary data, Section S.1.

We also tried to quantify the microbial influence on the observed processes by conducting additional batch experiments with sterilized soil. Unfortunately, both sterilization methods used (addition of formaldehyde and steam sterilization) induced massive changes in soil properties and already led to abiotic mobilization reactions, which made direct comparison with non-sterilized batches impossible. A detailed method description and results from sterile experiments can be found in Supplementary data, Section S.2.

Thus, we conducted an additional incubation experiment aiming at delivering a proof of principle for the correlation between microbial activity and Fe release in the soils used for this study. In

this additional incubation experiment, microbial activity was quantified by CO₂ production, a method that could not be used directly in the batch experiments which required specifically CO₂ addition. Both spring and summer soil were incubated with filtered river water in 50 mL septum vials at the same ratio as in the batch experiments but at a smaller scale (10 g soil + 15 mL water) and purged with N₂ for 1 h to generate anoxic conditions. Afterwards, the bottles were incubated in the dark at 12 °C (thermoelectric cool box), 21 °C (room temperature), and 35 °C (water bath) for 7 d. As in the batch experiments, the bottles were shaken daily. At the end of the incubation period, 4 mL were removed from the liquid phase with needle and syringe in an anoxic glovebox, 2 mL were stabilized in N₂-purged septum vials and stored overnight at 8 °C for analysis of dissolved CO₂, the remaining 2 mL were filtered (0.2 µm cellulose-acetate filter, CHROMAFIL® Xtra), and 1 mL was stabilized with 10 µL 8 M HNO₃ for total Fe analysis by ICP-MS.

2.4. Laboratory analysis

Total concentrations of Fe, Mn, As, and Cu were measured with a quadrupole ICP-MS (X-Series2, Thermo Scientific). Samples from the liquid phase were diluted with 0.16 M HNO₃, aqua regia digests from soil samples were diluted to a 1:10 dilution deionized water:aqua regia. Dilution factors were 1:10 for Mn, As, and Cu analysis, and between 1:10 and 1:10,000 for Fe analysis. Copper was measured in standard mode, As was measured in O₂ mode as AsO⁺, Fe and Mn were measured in KED mode (kinetic energy discrimination, –2 V for Mn, –3 V for Fe, with a mixture of 93% He and 7% H₂ as collision gas) to avoid polyatomic interferences. Rhodium was added as internal standard and internal drift correction was conducted by measuring a mid-range standard every 10 to 25 samples. We used TMDA-54.4 (National Water Research Institute, Environment Canada) as external reference material for quality control. A blank correction was conducted for the aqua regia digests. Calculated limits of detection (LOD) were 2.2 ± 4.4 µg L⁻¹ for Fe, 0.03 ± 0.06 µg L⁻¹ for Mn, 0.2 ± 0.1 µg L⁻¹ for As, and 0.16 ± 0.12 µg L⁻¹ for Cu.

Diluted CO₂ and CH₄ concentrations were calculated from head space concentrations in the septum vials using Henry's law. Gaseous head space concentrations were measured with a gas chromatograph (SRI Instruments 8610C, U.S.) equipped with a methanizer and a flame ionization detector.

Since a monitoring of nitrate and dissolved organic carbon (DOC) concentrations over the course of the experiment was not possible due to limited sample amount, these parameters were only determined for the initial river water as well as for the liquid phase directly after mixing with spring and summer soil in order to determine the amount of nitrate and DOC released from soil. Analysis of DOC was conducted by thermo-catalytic oxidation with a TOC-V_{CPN} Analyzer (Shimadzu) in undiluted, filtered (0.45 µm, nylon, CHROMAFIL® Xtra) samples, which had been stored at 8 °C for 5 days. Nitrate was determined with a Spectroquant® quick test (Nitrate Test Photometric, Merck) and a photometer (DR 2800, Hach-Lange), in undiluted, filtered (0.45 µm, nylon, CHROMAFIL® Xtra) samples, which had been stored frozen until analysis.

Three freeze-dried soil samples were investigated using Mössbauer spectroscopy including fresh spring soil, stored spring soil, and fresh summer soil, each before incubation. Within an anoxic glovebox (100% N₂), samples were prepared for Mössbauer spectroscopy by loading as dry, ground powders into Plexiglas holders (area 1 cm²). Samples were then transported to the Mössbauer instrument within airtight bottles which were only opened immediately prior to loading into a closed-cycle exchange gas cryostat (Janis cryogenics) to minimize exposure to air. Spectra were collected at 77 K and 5 K using a constant acceleration drive

system (WissEL) in transmission mode with a ⁵⁷Co/Rh source. All spectra were calibrated against a 7 µm thick α-⁵⁷Fe foil that was measured at room temperature. Analysis was carried out using Recoil (University of Ottawa) and the Voigt Based Fitting (VBF) routine (Rancourt and Ping, 1991). The half width at half maximum (HWHM) was constrained to 0.131 mm/s during fitting. The same soil samples were used for determination of oxalate- and dithionite-citrate-extractable pedogenic Fe(III) (oxyhydr)oxides, following the methods according to Schwertmann (1964) and Mehra and Jackson (1960), respectively. Total Fe and Aluminium (Al) concentrations in extracts were determined by ICP-MS in –2 V KED mode as described above. Two freeze-dried and ground samples from the initial spring and summer soil were analyzed in triplicate on total carbon and nitrogen content with a CHN elemental analyzer (Thermo Quest, Flash EA, 1112).

2.5. Calculations and statistics

In the differently treated batches (with/without CO₂, different temperatures) the loss of liquid due to evaporation varied strongly and measured dissolved concentrations had to be corrected according to the respective fluid loss. Evaporation was assumed to be constant over the course of the experiment, so the amount of liquid, remaining in the batches at a certain time step, could be calculated from weight difference before and after the experiment with a linear function, deducting fluid loss due to sampling.

Since data were not normally distributed, the Mann-Whitney-U-test was used to test for significance in differences between treatments, Kruskal-Wallis-test was used to test for significant trends over time, and Spearman's rank correlation was used to calculate correlation coefficients (*r_s*) and their significance level (*P*-value) between parameters (*α* = 0.05). All statistical analyses were done with R (R Development Core Team, 2008).

3. Results

3.1. Initial soil and water conditions

The physicochemical properties of the river water indicated that it could be used quite well as an analogue for an uncontaminated aquifer (Table 1). A comparison with the pore water of the reference site analyzed in Mehlhorn et al. (2014) showed that redox potential and Cu concentration were almost exactly the same (+390 mV and 3.3 µg Cu L⁻¹ for 30 cm depth in natural pore water) and Fe, Mn, and As concentrations were even considerably lower (2366 µg Fe L⁻¹, 179 µg Mn L⁻¹ and 22 µg As L⁻¹ in natural pore water). Only the pH of 8.6 in the river water was clearly higher compared to natural pore water (pH of 5.0 in pore water). This, however, did not affect the experiment, since pH in the batch reactors was mainly determined by soil pH (see Section 3.3). The properties of the water sampled in spring and in summer differed slightly. While redox potential and Fe concentration were slightly increased in summer, pH, Mn, and As concentrations were decreased.

Total element contents and pH of the soil used for batch experiments (Table 1) were similar to the soil samples from the reference site sampled and analyzed in 2013 (Mehlhorn et al., 2014). Differences between the soil sampled in spring and the one sampled in summer were already optically visible. The organic matter content, especially pronounced in fine root content, was clearly increased in the summer soil (total C content of 45 mg g⁻¹ compared to 20 mg g⁻¹ in spring soil) due to the course of vegetation period. Additionally, the soil was more porous and less moist. It is noteworthy that the total soil contents of Fe and As were lower by 39% and 45%, respectively, in summer soil compared to spring soil. The reduced Fe(III) (oxyhydr)oxide content was already

Table 1
Initial pH, redox potential, total element concentrations, C, N, DOC and nitrate (NO₃⁻) content in soils and/or river water. Soil pH was measured in 0.01 M CaCl₂ solution.

	pH	E _h [mV]	Fe [μg L ⁻¹]	Mn [μg L ⁻¹]	As [μg L ⁻¹]	Cu [μg L ⁻¹]	DOC [mg L ⁻¹]	C	NO ₃ ⁻ [mg L ⁻¹]	N
river, spring	8.6	380	167	91.8	4.2	3.3	3.4		14.6 ± 0.3	
river, summer	7.5	420	260	49.6	3.5	3.7	NA		NA	
			[mg g ⁻¹]	[μg g ⁻¹]	[μg g ⁻¹]	[μg g ⁻¹]		[mg g ⁻¹]		[mg g ⁻¹]
soil, spring	4.1		31.1	115	66.4	12.9		20		2
soil, summer	3.9		18.8	119	36.2	13.7		45		3

optically visible with less orange colored areas in summer compared to spring soil. Both oxalate- (Fe_o) and dithionite-citrate-extractable Fe (Fe_d) were significantly reduced in summer soil (Table 2) and an Fe_o/Fe_d ratio of 1.1 ± 0.2 compared to 0.7 ± 0.1 in fresh and 0.6 ± 0.0 in stored spring soil already indicated the absence of well-crystalline Fe phases. This difference seemed to be too high to be explained by soil heterogeneity alone. We therefore attributed these content decreases to a natural mobilization process due to higher microbial activity in summer soil, triggering reductive mineral dissolution processes. The content of oxalate-extractable Al ranged from 1.4 mg g⁻¹ in fresh spring soil to 2.0 mg g⁻¹ in fresh summer soil.

3.2. Iron phases identified by Mössbauer spectroscopy

3.2.1. Fresh spring soil

The spectrum collected at 77 K indicated that there was more than one Fe phase in the sample (Fig. 1a). The fitting parameters of the two sextets (denoted S1 and S2 in Supplementary data, Table S2) closely agreed to the values expected of goethite (Murad, 2010). The hyperfine field (B_{hf}), however, was different for each sextet which potentially suggests that there were two distinct types of goethite present with different particle sizes, i.e. the site with B_{hf} = 46 T was likely to have a smaller particle size than the site with B_{hf} = 49 T. Combined, these two crystalline sextets contributed to 24% of the total spectral area at 77 K. The three doublets which were also required for accurate fitting of the data had hyperfine parameters which corresponded to Fe(II) and Fe(III) phases. The doublet denoted D3 in Supplementary data, Table S2 was within an intermediate region which could not accurately be defined as either Fe(II) or Fe(III). The calculated amount of Fe(II) in the system was thus between 19 and 26%.

As the temperature was lowered to 5 K, the total area of the crystalline Fe component (sextet) increased as the sample underwent magnetic ordering. Again two sextets were used to fit this region, however, now the quadrupole splitting (ΔE_Q) was different between the two suggesting that we could no longer ascribe both sextets to goethite. A potential explanation is that as the temperature decreased, the hyperfine field of S1 increased and at 5 K could no longer be distinguished from S2. Now, only one sextet corresponded to goethite which was a combination of S1 and S2 from the 77 K spectrum. The new sextet, denoted S3 (Supplementary data, Table S2) accounts for 49% of the total spectral area, corresponds to

Table 2
Oxalate-extractable Fe (Fe_o) and Al (Al_o), dithionite-citrate-extractable Fe (Fe_d) and ratio Fe_o/Fe_d for the 3 different start soils given as mean ± standard deviation (triplicates).

	Fe _o [mg g ⁻¹]	Fe _d [mg g ⁻¹]	Fe _o /Fe _d	Al _o [mg g ⁻¹]
Spring soil, fresh	10.8 ± 0.5	16.6 ± 2.0	0.7 ± 0.1	1.4 ± 0.0
Spring soil, stored	14.2 ± 0.6	22.3 ± 1.3	0.6 ± 0.0	1.5 ± 0.1
Summer soil, fresh	7.6 ± 1.4	6.7 ± 0.3	1.1 ± 0.2	2.0 ± 0.0

a mineral phase which was not magnetically ordered at 77 K and is perhaps more likely to correspond to a short range ordered mineral such as ferrihydrite (Murad, 2010). Three doublets were still required to fit the data at 5 K which suggests they were either too small to undergo magnetic ordering, or more likely corresponded to sulfide minerals or perhaps phyllosilicates.

3.2.2. Stored spring soil

As expected, the main components for the stored spring soil were almost identical to fresh spring soil (Fig. 1b). There were some small differences in the relative abundances of the sextets, specifically an increase in the crystalline components such as goethite. This indicates that the samples underwent some crystallization during the 11 week storage period. If we combine the relative abundances for S1+S2 and S3 for both fresh and stored spring soils at 5 K, we see the total spectral areas were in fact identical. However, the stored spring soil showed a higher proportion of goethite, likely due to crystallization during storage.

3.2.3. Fresh summer soil

The Mössbauer spectra for the fresh summer soil showed some clear differences compared to both fresh and stored spring soil (Fig. 1c). This was especially true at 77 K where no sextets could be detected. This suggests there was little to no goethite present when the soil was collected during the summer. The three doublets used during the fitting of this spectrum shared very similar characteristics to the three doublets observed in fresh and stored spring soil indicating that all three samples shared the same parent material.

Two crystalline sextets were required during the fitting of the fresh summer soil at 5 K (S2 and S3). An additional poorly defined sextet (S1) was also required indicating that part of the sample was still not fully magnetically ordered at this temperature. Such behavior is indicative of small particle size, substitution of additional elements into the mineral (Chadwick et al., 1986; Murad and Cashion, 2004), or a strong association to organic matter (Chen et al., 2015). Based on the hyperfine parameters it was difficult to accurately determine the mineral phases corresponding to these sextets. It is possible that these sextets were also present for fresh and stored spring soils however, due to the presence of more dominant phases such as ferrihydrite and goethite, they could not be clearly distinguished. It should also be noted that it was not possible to determine the mineral identities of several of the Fe phases present in the samples and in some cases these unknown phases accounted for more than 50% of the relative spectral area of the Mössbauer spectra (Supplementary data, Table S2). Nevertheless, it appears that based on the 77 K and 5 K data major Fe components in the soils were short range ordered minerals (e.g. ferrihydrite or goethite).

3.3. Batch Experiment I: variation of temperature

While the dissolved CO₂ concentration in the control batches increased only slightly (to 0.6 ± 0.1 mmol L⁻¹ for C,

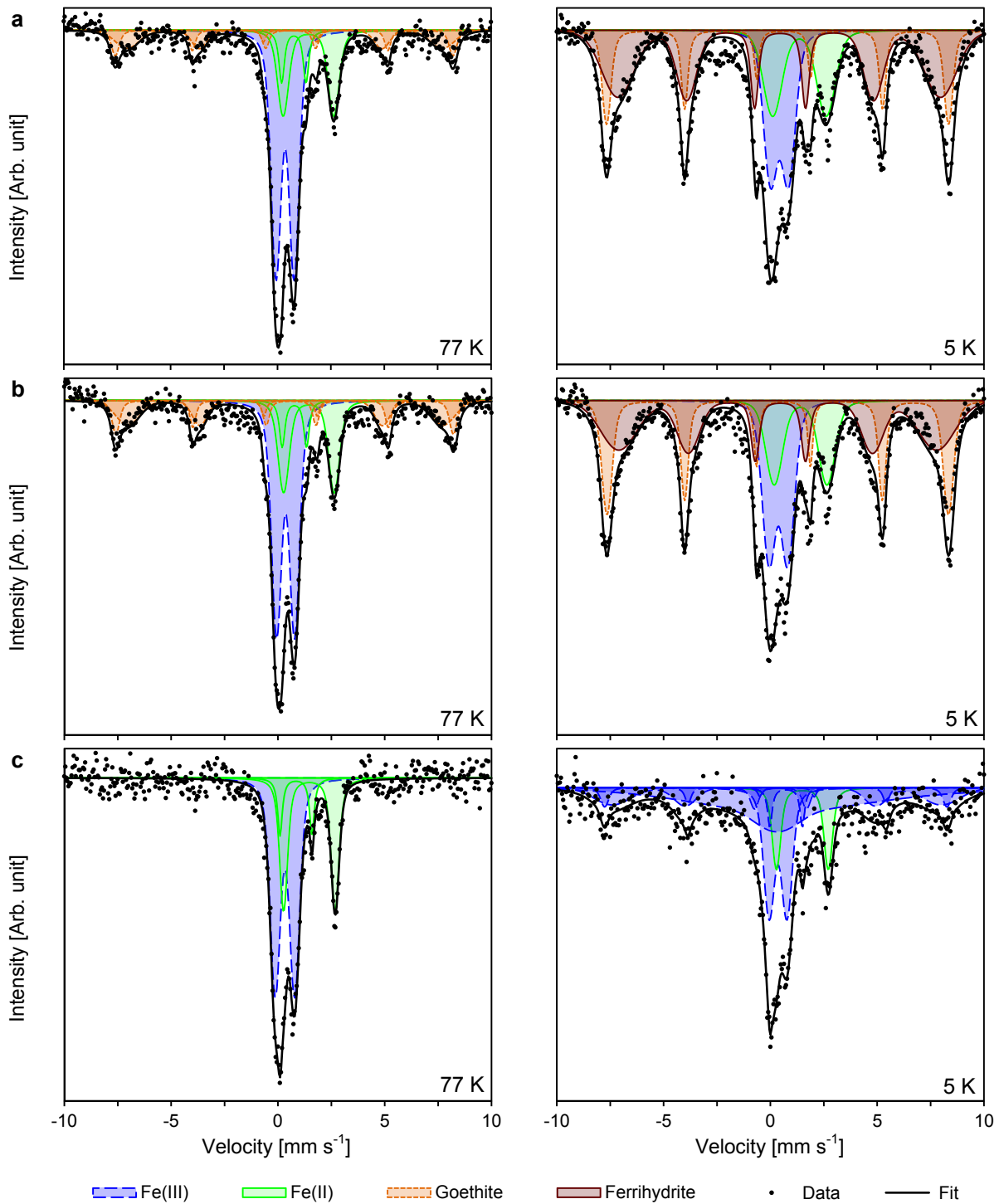


Fig. 1. Mössbauer spectra of fresh spring soil (a), stored spring soil (b), and fresh summer soil (c) each measured at 77 K (left) and 5 K (right).

$0.8 \pm 0.0 \text{ mmol L}^{-1}$ for RT, and $0.4 \pm 0.3 \text{ mmol L}^{-1}$ for H) compared to the initial river water (0.1 mmol L^{-1}), the batches with CO_2 treatment showed a strong increase (Supplementary data, Fig. S3). For the blank batches which only contained river water the dissolved CO_2 concentration increased in the order heated (H) < room temperature (RT) < cooled (C) ($17 < 23 < 29 \text{ mmol L}^{-1}$), as expected from the temperature dependency of the Henry's law constant, that predicts higher CO_2 solubility in colder water. For the batches with soil and CO_2 treatment, the cooled samples (C) showed again the

highest dissolved CO_2 concentration ($25 \pm 0.5 \text{ mmol L}^{-1}$), but batches RT and H were relatively similar (12 ± 1 , and $14 \pm 6 \text{ mmol L}^{-1}$, respectively), taking into account the high standard deviation for batches H. As expected, methane was not detected in any of the samples, since methanogenesis is thermodynamically very unlikely as long as high Fe(III) (oxyhydr)oxide concentrations are present.

The soil pH showed only a slight decrease during the course of the experiment, from initially 4.1 to 3.9 ± 0.1 . Since no difference

between different temperature treatments or between control and treatment could be observed, the decrease is probably caused by the mixing of soil and river water following desorption and dissolution reactions. The pH of the liquid phase showed a strong initial decrease both in batches with and without CO₂ treatment from 8.6 in river water to values between 4.4 and 5.2 within the first 1 h (Fig. 2a) that was caused by mixing with the already acidic soil. After this initial decrease, both controls and treatments remained at relatively constant pH for batches RT (controls: 4.9 ± 0.1 , treatments: 4.8 ± 0.1) and C (control: 5.0 ± 0.2 , treatments: 4.7 ± 0.1), but heated batches (H) showed a significant decrease ($P = 0.007$) in controls (from 5.0 ± 0.1 at 1 h to 4.3 ± 0.1 at 42 d) and increase ($P = 0.018$) in treatments (from 4.5 ± 0.1 at 1 d to 4.8 ± 0.1 at 42 d) over the course of the experiment. Comparison between different temperature treatments showed that pH in batches H was significantly lower than in batches RT ($P = 0.0003$) and C ($P = 0.011$), which contradicted the assumption, that higher CO₂ dissolution in batches C would cause a lower pH due to carbonic acid formation. Further processes like redox reactions seemed to buffer pH and prevent a further pH decrease.

After addition of river water to the soil, redox potential in the batches increased strongly within 1 h, both in controls (from +380 mV to +500 ± 10 mV in RT, +560 ± 10 mV in C, and +620 ± 0 mV in H) and treatments (to +560 ± 0 mV in RT, +570 ± 0 mV in C, and +610 ± 10 mV in H), probably caused by oxidizing soil constituents (Fig. 2b). During the course of the experiment, the controls stayed relatively constant at +570 ± 40 mV for RT, +590 ± 30 mV for C, and +570 ± 40 mV for H, while treatments showed a significant decrease, most pronounced for batches H (to +370 ± 10 mV, $P = 0.0037$), followed by RT (to +420 ± 10 mV, $P = 0.0062$) and C (to +480 ± 20 mV, $P = 0.016$), leading the soil towards more anoxic conditions. The decrease in redox potential hinted towards redox reactions that released reduced species into the pore water, thereby consumed protons and thus buffered pH, e.g., nitrate reduction and reductive dissolution of Fe(III) (oxyhydr)oxides. The order in redox potential decrease with H>RT>C might already be a hint towards stronger microbial activity at higher temperatures.

Mixing of river water with soil led to an initial concentration increase of nitrate (from 14.6 ± 0.3 to 32.8 ± 0.2 mg L⁻¹), DOC (from 3.4 to 4.0 mg L⁻¹), and all considered elements in the liquid phase within 1 h for both controls and treatments (except Fe treatments, data for As 1 h to 3 d (H) or 7 d (RT, C) are missing due to measurement problems) due to mixing with pore water and fast desorption of weakly bound ions (Fig. 2c–f). Calculated concentration increase factors X (Table 3) show that an increase in liquid phase concentration (end of experiment vs. river water blank) over the whole time of the experiment occurred for all elements both in controls and treatments, except for Fe controls and for As controls and treatments at batches RT and C. Observations for each individual element are described in detail as follows.

The highest increases in liquid phase concentrations were observed for Fe in CO₂ treatments (Table 3, Fig. 2c). After an initial “lag phase” of 1–3 d, in which concentrations changed only slightly, the concentration in the treatments increased almost linear from initially 0.2 mg Fe L⁻¹ to 3.2 ± 1.4 mg L⁻¹ in batches C (19 ± 9 fold increase), to 5.0 ± 1.6 mg L⁻¹ in RT (30 ± 9 fold increase), and 18.4 ± 4.0 mg L⁻¹ in H (111 ± 24 fold increase), while the controls showed no significant change of Fe over time and stayed relatively constant at 0.2 ± 0.1 mg L⁻¹ for C, 0.1 ± 0.1 mg L⁻¹ for RT, and 0.2 ± 0.1 mg L⁻¹ for H.

The mobilization behavior of Mn differed completely from that of Fe (Fig. 2d). Following the mixing of water and soil, all batches showed an increase in dissolved Mn concentration, slightly lower in controls (from 92 μg L⁻¹ in initial river water to 166 ± 15 μg L⁻¹ in C,

149 ± 12 μg L⁻¹ in RT, and 139 ± 6 μg L⁻¹ in H) compared to treatments (to 213 ± 6 μg L⁻¹ in C, 228 ± 6 μg L⁻¹ in RT, and 185 ± 2 μg L⁻¹ in H after 1 h). After this initial mobilization, the controls showed only a slight further increase of Mn in liquid phase concentration to 203 ± 12 μg L⁻¹ in batches C, 211 ± 15 μg L⁻¹ in RT, and 204 ± 20 μg L⁻¹ in H after 42 d. For the treatments, the strong Mn mobilization continued until 1 d with highest initial Mn mobilization for batches C (to 277 ± 12 μg L⁻¹), followed by RT (to 262 ± 14 μg L⁻¹), followed by H (to 218 ± 4 μg L⁻¹). For the rest of the experiment, the concentration of Mn in C treatments stayed relatively constant at 292 ± 28 μg L⁻¹, while RT treatments even showed a slight Mn re-immobilization to a final concentration only slightly above the respective controls (229 ± 27 μg L⁻¹). Only Mn in the H treatments continuously increased to 262 ± 40 μg L⁻¹ at d 42, but with a very low rate of 1.6 ± 1.3 μg kg_{soil}⁻¹ d⁻¹ and no significance ($P = 0.0868$).

Dissolved As concentration decreased in all control batches (from 4.2 μg L⁻¹ in initial river water to 2.5 ± 0.1 μg L⁻¹ in C, 2.6 ± 0.1 μg L⁻¹ in RT, and 2.5 ± 0.1 μg L⁻¹ in H) and also in the treatments for batches C (to 2.6 ± 0.7 μg L⁻¹) and RT (to 2.2 ± 0.4 μg L⁻¹) after 42 d (Fig. 2e). However, since a slight As concentration decrease at d 28 (to 3.8 ± 0.2 μg L⁻¹) and d 42 (3.4 ± 0.2 μg L⁻¹) was also observed in the water blanks (Supplementary data, Table S3), part of this As immobilization might be attributed to sensitivity changes during analysis (analysis of d 28 and d 42 samples in a separate run). Only the As concentrations in the heated batches with CO₂ exposure differed significantly from the related control ($P = 0.0007$) by showing a 1.5 ± 0.3 fold increase in As concentration up to 28 d (to 6.8 ± 1.6 μg L⁻¹) that was, however, not deemed as significant due to high standard variations ($P = 0.074$).

Copper is the only element where almost no differences between controls and treatments and between different temperature treatments could be detected (Fig. 2f). After an initial, immediate (1 h) Cu mobilization in both controls (from 3.3 μg L⁻¹ in initial river water to 11.1 ± 1.8 μg L⁻¹ in C, 7.9 ± 4.6 μg L⁻¹ in RT, and 6.5 ± 1.3 μg L⁻¹ in H) and treatments (to 5.9 ± 0.6 μg L⁻¹ in C, 5.7 ± 0.6 μg L⁻¹ in RT, and 6.6 ± 0.7 μg L⁻¹ in H), dissolved Cu concentrations in the different batches stayed relatively constant at values around 5.0–9.0 μg L⁻¹. Only the H treatment differed ($P = 0.0369$) from the respective control and showed a significant ($P = 0.0096$) change in Cu over time, with a continuous increase up to 10.9 ± 1.6 μg L⁻¹ until d 14 and a following decrease to 7.4 ± 1.0 μg L⁻¹ after 42 d.

Total solid phase contents did not show any change during the course of the experiment that was significantly higher than the natural variation in the soil (Supplementary data, Tables S4 and S5) which is probably due to the high pool of the considered elements in the soil compared to the small amounts mobilized into liquid phase.

3.4. Batch Experiment II: variation of start soil conditions

Both the batches with stored spring soil (H2) and the ones with fresh summer soil (H3) showed remarkable differences to the batches with fresh spring soil from Batch Experiment I (for better distinction hereafter referred to as H1) despite the similar temperature treatment (incubation at 35 °C).

As in Batch Experiment I, mixing of the filtered river water with soil caused a strong decrease in liquid phase pH for both controls and treatments (from 8.6 to values between 4.4 and 5.1 after 1 h–7 d, Fig. 3a). This initial pH decrease was followed by a slow increase in the treatments, with the fastest increase in the fresh summer soil H3 (to 4.8 ± 0.1 after 21 d, $P = 0.015$), followed by the fresh spring soil H1 (to 4.8 ± 0.1 after 42 d, $P = 0.018$) and slowest for the stored

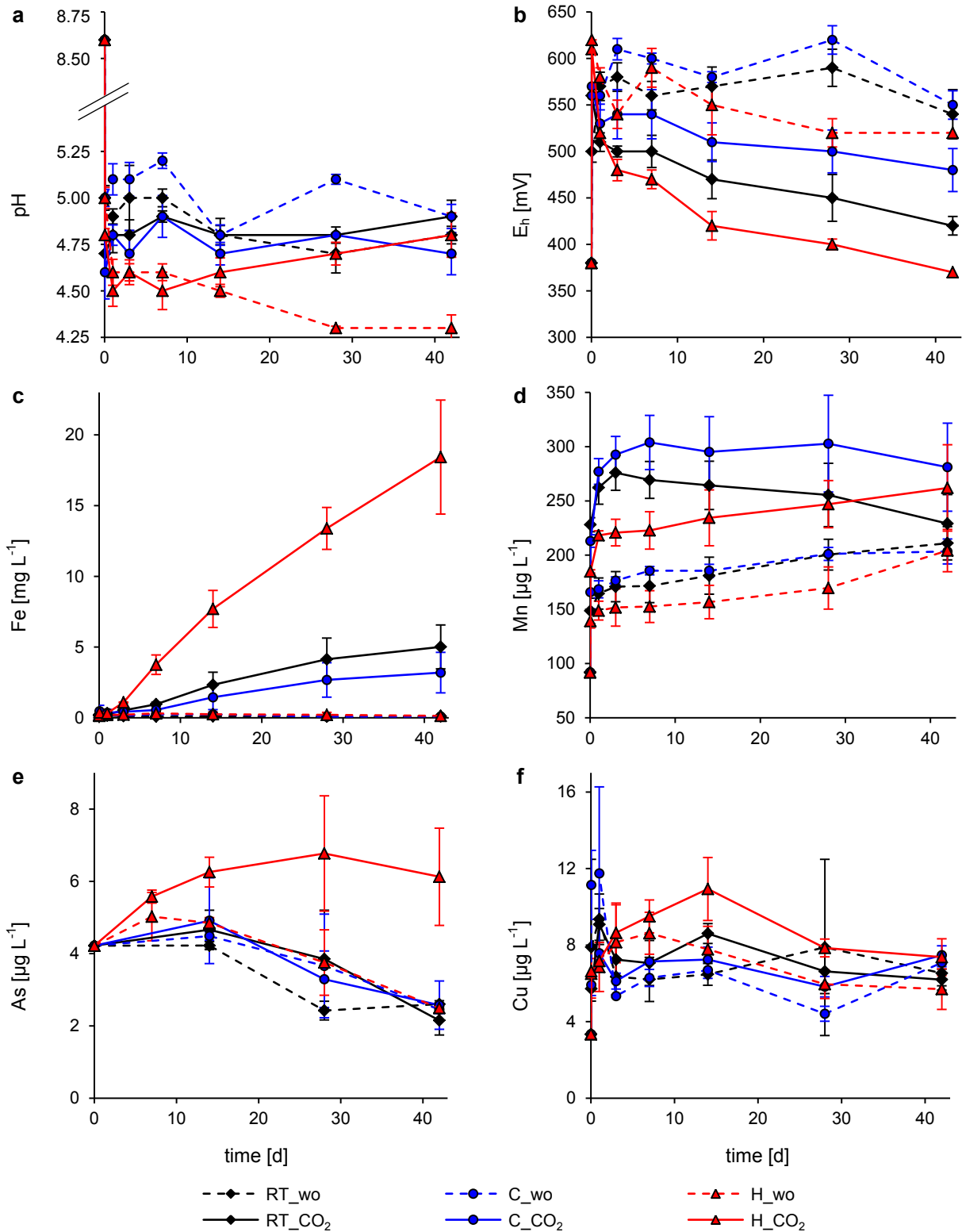


Fig. 2. Changes in liquid phase pH (a), redox potential (b), and total dissolved concentration (evaporation corrected) of Fe (c), Mn (d), As (e), and Cu (f) during Batch Experiment I with (solid line) and without (abbreviation “wo”, dashed line) CO₂ at room temperature (RT, 22 °C, black squares), cooled (C, 16 °C, blue circles), and heated (H, 35 °C, red triangles) in liquid phase. Data for As for 1 h - 3 d (H) or 7 d (RT, C) are missing due to measurement problems. Single outliers from triplicates had to be removed for the following data points, resulting in duplicates: H_wo_1h for Fe, RT_wo_d28 and H_CO₂_d3 for Cu. (For interpretation of the references to colour in this figure legend, the reader is referred to the web version of this article.)

spring soil H2 (to 4.6 ± 0.1 after 41 d, $P = 0.008$). A further increase was also observed for H3 controls (to 4.7 ± 0.1 after 21 d, $P = 0.009$,

while pH in H2 controls stayed relatively constant (at 4.6 ± 0.1 from 7 to 41 d) and H1 controls showed a significant decrease (to

Table 3

Factor X of concentration increase in liquid phase compared to day 0 and average daily mobilization rate r_{avg} for Batch Experiment I (3 different temperatures: cooled (C), room temperature (RT), and heated (H)) given as *mean ± standard deviation* (triplicates).

Element	Treatment	X-fold initial concentration [-]		r_{avg} [$\mu\text{g kg}_{soil}^{-1} \text{d}^{-1}$]	
		wo	CO ₂	wo	CO ₂
Fe	C	0.5 ± 0.3	19 ± 9	-2.9 ± 1.7	108 ± 51
	RT	0.6 ± 0.5	30 ± 9	-2.2 ± 2.8	173 ± 56
	H	0.8 ± 0.5	111 ± 24	-1.2 ± 2.8	652 ± 144
Mn	C	2.2 ± 0.1	3.1 ± 0.4	4.0 ± 0.4	6.8 ± 1.4
	RT	2.3 ± 0.2	2.5 ± 0.3	4.3 ± 0.5	4.9 ± 1.0
	H	2.2 ± 0.2	2.9 ± 0.4	4.0 ± 0.7	6.1 ± 1.4
As	C	0.58 ± 0.03	0.61 ± 0.16	-0.06 ± 0.00	-0.06 ± 0.02
	RT	0.62 ± 0.02	0.51 ± 0.10	-0.06 ± 0.00	-0.07 ± 0.01
	H	0.59 ± 0.03	1.45 ± 0.32	-0.06 ± 0.00	0.07 ± 0.05
Cu	C	2.1 ± 0.1	2.2 ± 0.1	0.13 ± 0.01	0.15 ± 0.02
	RT	2.0 ± 0.2	1.9 ± 0.2	0.11 ± 0.02	0.10 ± 0.02
	H	1.7 ± 0.3	2.2 ± 0.3	0.08 ± 0.04	0.14 ± 0.03

4.3 ± 0.1 at 42 d, $P = 0.007$). However, pH differences between controls and treatments were not significant. Again, a strong increase of redox potential after mixing of soil and river water within 1 h was observed (from +380 mV in H1 and H2 and +420 mV in H3 to +620 ± 10 mV in H1, +550 ± 10 mV in H2, and +540 ± 10 mV in H3, Fig. 3b). The initial increase was followed by a decrease in CO₂ treatments, that was strongest for the organic-rich batches H3 (to +340 ± 20 mV after 21 d, $P = 0.0058$), followed by the fresh spring soil H1 (to +370 ± 10 mV after 42 d, $P = 0.0037$) followed by the stored soil H2 (to +410 ± 20 mV after 41 d, $P = 0.0052$). The controls remained at significantly higher redox potentials over the course of the experiment (between +460 and +600 mV, $P < 0.0005$). The concentration increases of nitrate (from 14.6 ± 0.3 to 49.5 ± 0.3 mg L⁻¹) and DOC (from 3.4 to 6.1 mg L⁻¹) following mixing of soil and river water were also clearly higher for the organic rich summer soil compared to spring soil (increase to 32.8 ± 0.2 mg L⁻¹ for nitrate and to 4.0 mg L⁻¹ for DOC).

Same as for Batch Experiment I, an initial liquid phase concentration increase within 1 h was also observed in this experiment for most of the considered elements (Fig. 3c–f). Exceptions were As and Fe, that showed a slight initial decrease in the batches with summer soil (H3). Calculated concentration increase factors (X , Table 4) indicated that over the full experiment time (end of experiment vs. river water blank) liquid phase concentrations of all elements increased, with Fe and As controls being the only exceptions.

Again, the highest increase rates were observed for Fe in CO₂ treatments, with an average daily mobilization rate (r_{avg} , Table 4) of 0.3 ± 0.2 mg kg_{soil}⁻¹ d⁻¹ for treatments with stored spring soil (H2), 0.7 ± 0.1 mg kg_{soil}⁻¹ d⁻¹ for treatments with fresh spring soil (H1), and 1.9 ± 0.6 mg kg_{soil}⁻¹ d⁻¹ for treatments with fresh summer soil (H3), while controls stayed relatively constant at 0.28 ± 0.32 mg L⁻¹ for batches H1, 0.32 ± 0.42 mg L⁻¹ for H2, and 0.24 ± 0.13 mg L⁻¹ for H3 (Fig. 3c). However, clear Fe mobilization only began after an initial lag phase of 3 d for batches H1 and H2 and 1 d for batches H3. Final dissolved Fe concentrations in the treatments were 7.95 ± 5.67 mg L⁻¹ after 41 d in batches H2, 18.43 ± 4.03 mg L⁻¹ after 42 d in H1, and 26.33 ± 7.80 mg L⁻¹ after 21 d in H3.

The Mn mobilization pattern was similar to Batch Experiment I with a shift in mobilization rate within the first 24 h (Fig. 3d). Following mixing of soil and river water, a fast increase in dissolved Mn concentration occurred, again slightly higher in treatments (from 92 μg L⁻¹ to 218 ± 4 μg L⁻¹ for H1, to 206 ± 6 μg L⁻¹ for H2, and from 50 μg L⁻¹ to 185 ± 9 μg L⁻¹ for H3) compared to controls

(to 149 ± 9 μg L⁻¹ for H1, to 153 ± 4 μg L⁻¹ for H2, and to 131 ± 3 μg L⁻¹ for H3). But while in the experiment with fresh spring soil (H1) the average liquid phase concentration of Mn in the treatments further increased over the remaining experiment time, even at a very low rate (to 262 ± 40 μg L⁻¹ after 42 d), the treatments of H2 and H3 showed a slight re-immobilization of Mn (final concentrations of 159 ± 28 μg L⁻¹ after 41 d in H2 and 164 ± 10 μg L⁻¹ after 21 d in H3). The Mn concentration of the controls stayed relatively constant for the rest of the experiment at 160 ± 24 μg L⁻¹ in batches H1, 157 ± 20 μg L⁻¹ in H2, and 134 ± 19 μg L⁻¹ in H3. Only the controls of H1 and H2 showed a Mn concentration increase at the last sampling day (to 204 ± 20 μg L⁻¹ in H1 and 193 ± 16 μg L⁻¹ in H2), leading even to a higher final dissolved Mn concentration in controls compared to treatments for H2.

Arsenic had shown a 1.5 ± 0.3 fold concentration increase in the liquid phase of the treatments with fresh spring soil (H1), however, after storage of the soil for 11 weeks (H2) the repetition of the batch experiment led to no As mobilization at all (liquid phase As concentration of 3.55 ± 0.90 μg L⁻¹ over the whole experiment, Fig. 3e). The same effect was observed for the controls of H1 and H2 which even showed a slight immobilization (from 4.2 μg L⁻¹ to 2.5 ± 0.1 μg L⁻¹ after 42 d for H1 and to 2.0 ± 0.03 μg L⁻¹ after 41 d for H2). The extreme As mobilization in treatments with fresh summer soil (H3) was particularly remarkable. Liquid phase As concentration increased significantly from 3.5 μg L⁻¹ to 55.9 ± 24.7 μg L⁻¹ after 21 d ($P = 0.0088$), despite the high variation between the triplicates. The mobilization seemed to occur within the first 7 d, while As concentration stayed relatively constant afterwards. However, this impression is biased by one of the triplicate samples, that showed an extremely high As mobilization to up to 97.6 μg L⁻¹ on day 7, followed by a further decrease to 81.3 μg L⁻¹ on day 21 (compare Supplementary data, Fig. S4). The other 2 treatment batches showed a continuous increase over the course of the experiment. Like Fe mobilization in treatments of H3, liquid phase concentration increase of As only started after >1 d and As and Fe concentrations correlated significantly ($r_S = 0.95$, $P = 0$).

Copper was again the element with the smallest differences between controls and treatments (Fig. 3f). An initial Cu mobilization within 1 h occurred in both controls and treatments, following the mixing of filtered river water and soil, that was highest for batches H3 (from 3.7 μg L⁻¹ to 9.0 ± 0.6 μg L⁻¹, compared to a Cu increase from 3.4 μg L⁻¹ to 6.6 ± 0.5 μg L⁻¹ in H1 and to 6.5 ± 1.6 μg L⁻¹ in H2). Batches with stored spring soil (H2) showed a Cu mobilization over the course of the experiment for both controls and treatments. However, the relatively high Cu concentrations on days 28 and 41 are probably caused by analysis problems, since the water blank sample without soil showed the same increase (Supplementary data, Table S3). Differences between H2 controls and treatments were not significant. The batches with fresh summer soil showed a completely different behavior than batches H1 and H2 with significant differences between controls and treatments ($P = 0.0304$): while the controls stayed relatively constant at 9.4 ± 2.2 μg L⁻¹ after initial mobilization, the treatments showed an increase to 10.9 ± 0.1 μg L⁻¹ at day 1, followed by a further decrease to 6.2 ± 1.1 μg L⁻¹ at day 21. An immobilization process for Cu seemed to have occurred in CO₂ treatments.

4. Discussion

4.1. Soil processes following exposure to CO₂

When a CO₂ outgassing builds up in a redoximorphic Fluvisol, due to the formation of a mofette or leakage from a GCS site, CO₂ will dissolve in the pore water and form carbonic acid. According to

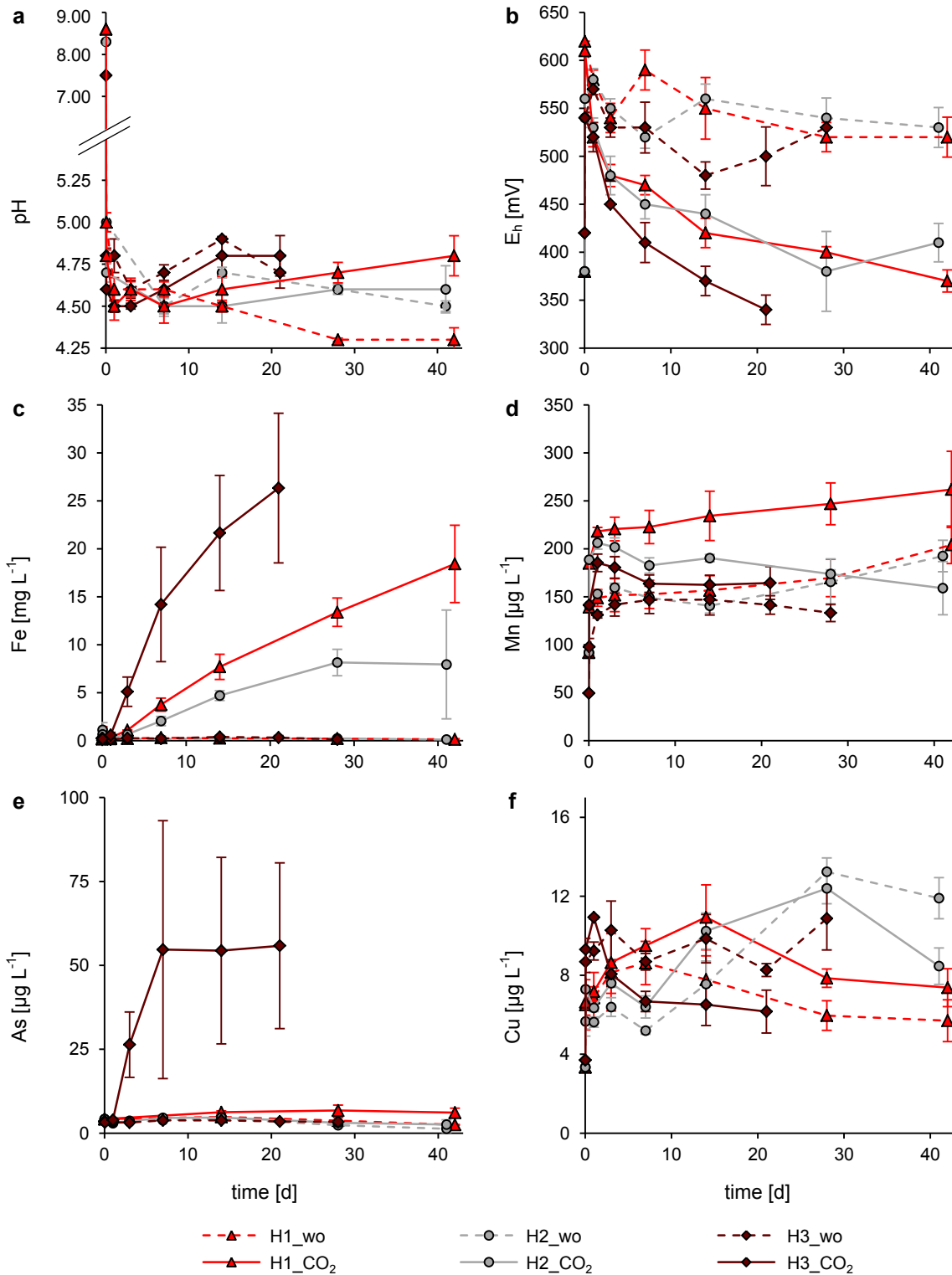


Fig. 3. Changes in liquid phase pH (a), redox potential (b), and total dissolved concentration (evaporation corrected) of Fe (c), Mn (d), As (e), and Cu (f) during Batch Experiment II with (solid line) and without (abbreviation “wo”, dashed line) CO₂ at 35 °C with 3 different start soil conditions (H1: fresh spring soil from Batch Experiment I, red triangles, H2: stored spring soil, grey circles, H3: fresh summer soil, dark red squares) in liquid phase. Note the change in scaling after y-axis break in (a); pH data for H2 are missing on 1 d and 3 d due to electrode calibration problems. Data for As 1 h – 3 d are missing for H1 due to measurement problems. Single outliers from triplicates had to be removed for the following data points, resulting in duplicates: H3_wo_d7 for Fe, Mn, and Cu, H2_wo_d41 and H3_wo_d3 for As, H1_CO₂_d3 for Cu. (For interpretation of the references to colour in this figure legend, the reader is referred to the web version of this article.)

Henry's Law, more CO₂ will dissolve in colder water, as could be verified in Batch Experiment I with different temperature

treatments. However, the dissolution of CO₂ did not cause a significant pH decrease in our experiments as has been observed in

Table 4

Factor X of concentration increase in liquid phase compared to day 0 and average daily mobilization rate r_{avg} for Batch Experiment II (3 different “start” soil conditions, ordered according to mobilization rates: stored spring soil (H2), fresh spring soil (H1), and fresh summer soil (H3)) given as *mean* \pm *standard deviation* (triplicates).

Element	Soil	X-fold initial concentration [-]		r_{avg} [$\mu\text{g kg}_{\text{soil}}^{-1} \text{d}^{-1}$]	
		wo	CO ₂	wo	CO ₂
Fe	H2	0.7 \pm 0.3	48 \pm 34	-1.9 \pm 1.7	285 \pm 207
	H1	0.8 \pm 0.5	111 \pm 24	-1.2 \pm 2.8	652 \pm 144
	H3	0.5 \pm 0.0	101 \pm 30	-7.2 \pm 0.4	1862 \pm 557
Mn	H2	2.1 \pm 0.2	1.7 \pm 0.3	3.7 \pm 0.6	2.5 \pm 1.0
	H1	2.2 \pm 0.2	2.9 \pm 0.4	4.0 \pm 0.7	6.1 \pm 1.4
	H3	2.7 \pm 0.2	3.3 \pm 0.3	4.5 \pm 0.5	8.2 \pm 1.2
As	H2	0.31 \pm 0.26	0.61 \pm 0.33	-0.08 \pm 0.01	-0.06 \pm 0.05
	H1	0.59 \pm 0.03	1.45 \pm 0.32	-0.06 \pm 0.00	0.07 \pm 0.05
	H3	0.96 \pm 0.00	15.9 \pm 7.0	-0.01 \pm 0.00	3.74 \pm 1.76
Cu	H2	3.6 \pm 0.3	2.5 \pm 0.3	0.31 \pm 0.04	0.19 \pm 0.03
	H1	1.7 \pm 0.3	2.2 \pm 0.3	0.08 \pm 0.04	0.14 \pm 0.03
	H3	2.9 \pm 0.4	1.7 \pm 0.3	0.38 \pm 0.09	0.18 \pm 0.08

numerous other batch studies (e.g. Kirsch et al., 2014; Lawter et al., 2015, 2016; Little and Jackson, 2010; Lu et al., 2010; Shao et al., 2015; Smyth et al., 2009). One reason for this is the already acidic Fluvisol used in this study. Mixing of river water and soil alone decreased the liquid phase pH to 4.5–5.0 in both controls and treatments. These pH values are in accordance with the pore water pH at the natural mofette site (Beulig et al., 2015; Mehlhorn et al., 2014). Since only slight changes in liquid phase pH occurred over the course of the experiment, despite the continuous supply of CO₂ in treatments and therefore a supply of protons, processes that buffer pH must have taken place. At a soil pH of 4.1 or 3.9, the buffer systems of silicates and cation exchange should be depleted and Aluminum and Fe(III) (oxyhydr)oxides are defined as the most important buffer systems at pH < 4.2 (Blume et al., 2016). Oxalate extraction indicated the presence of Al (hydr)oxides (1.4–2.0 mg g⁻¹) which might have contributed to buffer reactions. However, a screening of total dissolved Al concentration for 1 h vs. end-of-experiment samples revealed that no significant Al mobilization occurred in our experiments (data not shown), thus, Al (hydr)oxides were not dissolved. The initial fast drop in pH could have been caused by the rapid mobilization of dissolved organic matter (DOM) from soil by mixing with river water, indicated by increased DOC concentrations (increased by 19% after mixing with spring soil and by 81% after mixing with summer soil), initiating microbial processes, as observed in Porsch et al. (2014). Interestingly, the lowest liquid phase pH occurred in the heated batches H which contradicts the assumption of a lower CO₂ dissolution at higher temperatures. Since the heated, non-CO₂-treated control setups showed an even further pH decrease over the course of the experiment, the low pH might be caused by additional CO₂ release into the liquid phase from microbial respiration processes or production of fatty acids from microbial fermentation processes which should be highest in heated batches where temperature is within optimum range of many mesophilic bacteria. Unfortunately, no direct proof of fatty acid production was possible during this study due to limited sampling amount, but the presence of fermenting bacteria at the soil sampling site was recently demonstrated by Beulig et al. (2016). The pH increase in H treatments following the initial decrease might be caused by microbially enhanced proton consuming reactions like the reductive dissolution of Fe(III) (oxyhydr)oxides (Lions et al., 2014).

Relatively high redox potentials of +500 to +620 mV were measured in both controls and CO₂-treatments right after mixing of soil and river water. They were caused by the initially relatively

high oxygen content. The redox potential decrease during the course of the experiment, which could be observed in the CO₂ treatments, was most likely caused by microbial consumption of oxidizing compounds. The anoxic conditions caused by CO₂ purging forced heterotrophic microbes to use electron acceptors with less and less energy yield. While in the first 3 d, there was probably still oxygen available for aerobic respiration and the decrease in redox potential was relatively fast, the much slower decrease following day 3 indicates that heterotrophic microorganisms had switched to another respiration process. This process was most probably microbial Fe(III) reduction to Fe(II) coupled to Fe(III) (oxyhydr)oxide dissolution which is evidenced by the highly significant negative correlation between redox potential and dissolved total Fe concentration calculated with data from all experiments ($r_S = -0.74$, $P < 10^{-10}$). Additionally, fermentation has to be taken into account as possible microbial process under anoxic conditions that might both influence the pH by production of fatty acids and could also contribute indirectly to the reductive dissolution of Fe(III) (oxyhydr)oxide via electron shuttling (Benz et al., 1998; Kappler et al., 2004). The lowest final redox potentials were achieved in heated treatments with +370 \pm 10 mV for batches H1 and +340 \pm 20 mV for H3. However, these values were still higher than the redox potential measured in natural pore water of mofettes (+270 \pm 50 mV and +310 \pm 10 mV), but similar to those measured in pore water from references (+360 \pm 40 mV and +390 \pm 20 mV) (Mehlhorn et al., 2014). An influence of oxygen on the measured redox potential could not completely be ruled out, since the measurement had to be conducted under atmospheric conditions. However, the observed decrease in redox potential and the similarity between lab and field values indicated that artefact effects are probably negligible.

4.2. Mobility of Fe, Mn, As, and Cu following CO₂ exposure

Looking at the mobility of the metal(loid)s considered in this study, experiments with different temperature treatments allowed a clear distinction between two mobilization processes: at first the abiotic desorption of metal cations due to increasingly positively charged surfaces or competition with DOM released after mixing of soil and water phase and later the release of elements due to microbially-triggered dissolution of Fe(III) (oxyhydr)oxides and co-release of incorporated elements (Borch et al., 2009). The process of mobilization via desorption was relatively fast with main mobilization occurring within the first 3 d. Cooled treatments showed the highest mobilization rates, since more CO₂ was dissolved compared to warmer batches. The second, microbially-triggered mobilization process did not start until day 3 when all remaining oxygen was depleted and the microbes had to switch to the less favorable electron acceptor Fe(III). The generally higher mobilization rates for heated and organic-rich treatments provide evidence for a microbial nature of this process. Observations for the individual elements will be discussed in detail in the following section.

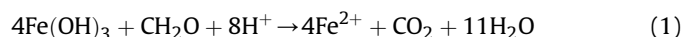
4.2.1. Iron

The results of our study suggest that the dissolution of Fe(III) (oxyhydr)oxides is the most pronounced mobilization process that occurs in an Fe-rich Fluvisol after a CO₂ outgassing event. The dominating Fe phases in the soils used for this study were identified to be goethite and ferrihydrite as well as some non-crystalline Fe(II) and Fe(III) phases (Section 3.2). Since we observed significantly increased Fe mobilization rates at higher incubation temperatures ($C < RT < H$) and an increased mobilization in the organic-rich summer soil (H2 < H1 < H3), we attributed this release to the microbially-triggered process of Fe(III) (oxyhydr)oxide reduction (Melton et al., 2014). The presence of Fe(III)-reducing bacteria was

proven by determination of most probable numbers (MPN) and revealed that $4.7 \cdot 10^4$ to $1.0 \cdot 10^6$ MPN mL⁻¹ of Fe(III)-reducing microorganisms were present in the spring soil (compare Supplementary data, Section S.1). However, no significant change in MPNs of heterotrophic aerobic, Fe(III)-, and sulfate-reducing bacteria could be detected in spring soil after incubation without/with CO₂ indicating that the relatively short experiment time of 6 weeks did not alter the microbial soil community, but only the activity of certain microbes, or that the changes were within the error of the MPN method. All attempts to quantify the microbial share on mobilization processes by comparison with data from sterilized batches were not successful: both sterilization with formaldehyde and via steam sterilization led to strongly increased mobilization rates for all considered elements (Supplementary data, Section S.2). Alteration of soil properties due to different sterilization methods is a well-known problem (Trevors, 1996 and references therein), especially in organic-rich soils (Berns et al., 2008). We thus concluded that sterilization of the natural soil used in this study was not suitable, since soil properties were influenced gravely and no comparability to the unaltered soil was given.

However, to further validate the activity of Fe(III)-reducing bacteria as main factor for Fe mobilization, we conducted an anoxic, 1 week-lasting post-study in which we quantified microbial activity by CO₂ production and correlated it with total Fe concentrations in the liquid phase, incubation temperature, and start soil (see Section 2.3 for detailed method description and Supplementary data, Section S.8 for detailed results). For both soils used (spring and summer soil), we found significant correlations between temperature treatment and CO₂ production (for both soils: $r_S = 0.96$, $P = 0.0028$) as well as between CO₂ production and Fe mobilization (spring soil: $r_S = 0.94$, $P = 0.0048$; summer soil: $r_S = 0.83$, $P = 0.0416$). The higher microbial activity in the organic-rich summer soil could also be verified with this experiment: CO₂ production in the summer soil was 2.4 ± 0.5 times higher compared to the spring soil and Fe mobilization was up to 9.7 ± 0.7 times higher (35 °C) leaving no doubt about the role of Fe(III)-reducing microbes on Fe mobilization. An additional factor for increased mobilization in summer soil was probably also the absence of crystalline Fe phases in summer soil and therefore a higher share of poorly-crystalline minerals (see Sections 3.1 and 3.2) that are more easily accessible for microbes (Cornell and Schwertmann, 2003; Porsch et al., 2014). The significantly decreased Fe mobilization in batches with stored spring soil (H2) can vice versa be explained by increased crystallinity of the Fe(III) (oxyhydr)oxides present in soil, as shown for goethite by Mössbauer spectroscopy and by increased Fe_d content.

This study provides evidence that a microbially-triggered, reductive dissolution of Fe(III) (oxyhydr)oxides can occur in CO₂ influenced soils, even if the redox potential is above the generally assumed threshold of +150 mV at neutral conditions (Blume et al., 2016). The reason for this is that the energy yield of microbial Fe(III) reduction increases with decreasing pH, since protons are consumed (Eq. (1)).



While the standard redox potential of Fe(II)/Fe(III) at pH 7 is -112 mV for a 1 mM Fe(II) solution, it is increased to +330 mV at pH 4.5 (Stumm et al., 1996). Kirk et al. (2013) observed that the activity of Fe(III)-reducing microorganisms surpassed that of sulfate-reducers at CO₂ partial pressures of 1 atm. They contributed this to increased proton concentrations (accompanied by a lowered pH) due to the dissociation of the carbonic acid formed and thus, a thermodynamic advantage of Fe(III)-reducers over sulfate-reducers. MPNs showed that sulfate-reducing bacteria were also

present in the soil used in this study (Supplementary data, Table S1). However, their activity must have been low, since most of the sulfur (S) mobilization in the treatments occurred within the first day and in the order C>RT>H (Supplementary data, Fig. S5). Thus, S mobilization was most likely caused by desorption reactions. Only the treatments of H1 (fresh spring soil) and H3 (fresh summer soil) showed a 2.2 ± 0.4 fold and 1.6 ± 0.1 fold concentration increase, respectively. However, since these were also the treatments with the highest Fe mobilization, the correlating S mobilization (H1: $r_S = 0.97$, $P = 0$; H3: $r_S = 0.93$, $P = 1.38 \cdot 10^{-9}$) might also be contributed to a co-release from Fe(III) (oxyhydr)oxide dissolution and not to direct microbial sulfate reduction.

4.2.2. Manganese

A sequential extraction procedure conducted with natural mofette and reference soil in 2013 detected most of the Mn in the non-specifically adsorbed fraction or bound to Fe(III) (oxyhydr)oxides, while Mn oxides were not detected (Mehlhorn et al., 2014). This is in good agreement with the mobilization processes we observed for Mn in the CO₂ treatments. Two different processes could be clearly distinguished: within the first 24 h, a fast and strong Mn mobilization occurred with initial mobilization rates r_{initial} increasing in the order H<RT<C (Table 5). This mobilization was caused by desorption of weakly bound Mn due to the increasing competition with protons, that was higher at lower temperatures, where more CO₂ could dissolve. The same pattern could be observed in the controls that were not treated with CO₂, but to a significantly lower extent. However, total differences between different temperature treatments were small, thus, an effect of soil heterogeneity cannot completely be ruled out. A further hint towards an abiotic desorption process was that in Batch Experiment II the heated batches showed quite similar initial mobilization rates (Table 5), despite the different start soil conditions. Similar patterns of Mn mobilization were also observed in other batch or field scale CO₂ studies (Lawter et al., 2016; Little and Jackson, 2010; Lu et al., 2010; Shao et al., 2015) and mainly attributed to co-release from calcite or dolomite dissolution. This process is unlikely in our study since these minerals are not stable under the acidic soil conditions and abiotic desorption must have been the dominating Mn mobilization process. The fast desorption stopped after at maximum 3 days when all weakly bound Mn was desorbed. Afterwards, the dissolved Mn concentration stayed relatively constant, or even decreased slightly (compare final mobilization rates r_{final} in Table 5; shift from r_{initial} to r_{final} is designated as “transition day”). One reason for the slight resorption of Mn could be the proton consumption by microbially-triggered Fe(III) (oxyhydr)oxide dissolution, decreasing competition for sorption sites. H1 treatments were the only batches, which showed a positive r_{final} of $1.6 \pm 1.3 \mu\text{g kg}_{\text{soil}}^{-1} \text{d}^{-1}$, however, with a very high standard variation. The Mn concentrations following day 3 correlated with Fe ($r_S = 0.71$, $P = 0.003$), which is a hint towards a Mn co-release from Fe(III) (oxyhydr)oxide dissolution that surpassed Mn resorption. Overall, the Mn mobilization in the CO₂ treatments was negligible when compared with the controls.

4.2.3. Arsenic

Sequential extraction in Mehlhorn et al. (2014) revealed that in reference soils from the Czech sampling site the biggest portion of As was adsorbed to or incorporated in poorly crystalline Fe(III) (oxyhydr)oxides. The reductive dissolution of Fe(III) (oxyhydr)oxides that we observed in the CO₂ treatments of the batch experiments should thus have led to an according As co-release. However, such an As co-release could only be observed in the heated treatments H1 and H3. In H1 treatments, an As mobilization up to 14 d could be observed ($r_{\text{initial}} = 0.22 \pm 0.04 \mu\text{g kg}_{\text{soil}}^{-1} \text{d}^{-1}$, Table 5), that

Table 5
Initial ($r_{initial}$) compared to final daily mobilization rates (r_{final}) for Batch Experiment I (3 different temperatures: cooled (C), room temperature (RT), heated (H)) and Batch Experiment II (3 different start soil conditions, ordered according to mobilization rates: stored spring soil (H2), fresh spring soil (H1), and fresh summer soil (H3)) given as *mean* \pm *standard deviation* (triplicates) for elements with a sharp shift in mobilization rate (Mn and As). The “transition day” between initial and final rate was determined optically from changes in element concentration in liquid phase over time.

Element	Treatment	Transition day	$r_{initial}$ [$\mu\text{g kg}_{\text{soil}}^{-1} \text{d}^{-1}$]		r_{final} [$\mu\text{g kg}_{\text{soil}}^{-1} \text{d}^{-1}$]	
			wo	CO ₂	wo	CO ₂
Mn	C	1	115 \pm 12	278 \pm 18	1.3 \pm 0.6	0.1 \pm 1.1
	RT	1	109 \pm 22	256 \pm 23	1.7 \pm 0.4	-1.2 \pm 0.4
	H	1	86 \pm 13	190 \pm 6	2.0 \pm 0.4	1.6 \pm 1.3
As	C	14	0.03 \pm 0.01	0.07 \pm 0.13	-0.11 \pm 0.01	-0.13 \pm 0.03
	RT	14	0.00 \pm 0.01	0.05 \pm 0.06	-0.09 \pm 0.01	-0.13 \pm 0.02
	H	14	0.07 \pm 0.02	0.22 \pm 0.04	-0.13 \pm 0.01	-0.01 \pm 0.05
Mn	H2	1	92 \pm 5	172 \pm 10	1.5 \pm 0.5	-1.8 \pm 1.1
	H1	1	86 \pm 13	190 \pm 6	2.0 \pm 0.4	1.6 \pm 1.3
	H3	1	122 \pm 5	204 \pm 14	0.1 \pm 0.6	-1.6 \pm 0.8
As	H2	7	-0.08 \pm 0.01	0.07 \pm 0.17	-0.08 \pm 0.01	-0.09 \pm 0.03
	H1	14	0.07 \pm 0.02	0.22 \pm 0.04	-0.13 \pm 0.01	-0.01 \pm 0.05
	H3	7	0.06 \pm 0.04	10.97 \pm 8.23	-0.03 \pm 0.01	0.12 \pm 1.62

correlated significantly with Fe mobilization ($r_s = 0.78$, $P = 2.5 \cdot 10^{-7}$). In the fresh summer soil of H3 treatments, the As mobilization occurred mainly within the first 7 days and was significantly higher than in H1 ($r_{initial} = 11 \pm 8 \mu\text{g kg}_{\text{soil}}^{-1} \text{d}^{-1}$). Here, too, As and Fe concentrations correlated significantly ($r_s = 0.95$, $P = 0$), but while in batches H1 a 111 \pm 24 fold Fe concentration increase caused a 1.5 \pm 0.3 fold As concentration increase, it was 101 \pm 30 fold for Fe vs. 16 \pm 7 fold for As in batches H3. This almost 10 times higher As mobilization in H3 despite a similar total Fe mobilization could either be caused by a different As content of the Fe(III) (oxyhydr)oxides in the start soil or by a differing resorption behavior. We would rate differences in As content of Fe(III) (oxyhydr)oxides as unlikely since both total As and total Fe concentration in the summer soil were decreased in the same order of magnitude, by 45 and 39%, respectively, compared to the spring soil (Table 1). This indicates that abiotic resorption of released As to positively charged soil surfaces must have been higher in spring compared to summer soil. Arsenic speciation measurements in pore water from the mofette site in Mehlhorn et al. (2014) revealed that most of the dissolved As is present as arsenite followed by arsenate. In the study presented here, As speciation analyses were not successful due to low total As concentrations. However, we assume arsenite and arsenate to be the dominant dissolved As species, since methylation or thioarsenates seem unlikely because no CH₄ formation and no significant S mobilization were observed. At the pH values observed in this study, arsenate should be present as negatively charged H₂AsO₄⁻ and arsenite as uncharged H₃AsO₃ (Cullen and Reimer, 1989). Most soil constituents, especially Fe(III) (oxyhydr)oxides, have a net-positive surface charge at the pH values measured in this study (e.g. points of zero charge (pH_{PZC}) are around 7.8–7.9 for ferrihydrite and 7.5–9.5 for goethite (Cornell and Schwertmann, 2003)), thus, the negatively charged arsenate has a high tendency to adsorb to these positively charged surfaces. Also, arsenite is known to have a high affinity to Fe(III) (oxyhydr)oxides, even at relatively low pH (Dixit and Hering, 2003; Goldberg and Johnston, 2001; Raven et al., 1998). Therefore, resorption to remaining Fe(III) (oxyhydr)oxide surfaces is the most likely re-immobilization process for As in the conducted batch experiments. Total Fe(III) (oxyhydr)oxide content in the spring soil was significantly higher than in the summer soil, thus, more resorption sites were available for released As, which could be one factor for the observed discrepancy in As mobilization. Another reason for a decreased resorption in the fresh summer soil of H3 could be the increased organic content. Dissolved organic matter and As can be

competitors for soil sorption sites (e.g. Bauer and Blodau, 2006; Redman et al., 2002). It is thus very likely that less As was re-immobilized in H3 since DOM covered most of the positively charged surfaces and less free sorption sites were available, resulting in a higher As net-mobilization. Additionally, As might have formed colloids or dissolved complexes with DOM and Fe (Bauer and Blodau, 2009; Ritter et al., 2006; Sharma et al., 2010, 2011), increasing its mobility in the organic rich summer soil. Competition between As and phosphate or between As and carbonate should have been of minor importance since no significant phosphorous mobilization was observed (data not shown) and carbonate was shown to be a weak competitor towards As under increased $p(\text{CO}_2)$ by Brechbühl et al. (2012).

In the RT and C batches, no net As-mobilization was observed. Arsenic resorption surpassed the significantly lower release from Fe(III) (oxyhydr)oxide dissolution. The stored spring soil H2 also did not show any As mobilization in the CO₂ treatments. The significantly decreased dissolution of Fe(III) (oxyhydr)oxides must have released less As compared to the fresh spring soil, that could all immediately resorb to other surfaces, resulting in no net-mobilization.

4.2.4. Copper

The main reason for focusing our study on the element Cu was that it seemed to be less mobile in natural mofettes compared to the respective reference sites as shown in Mehlhorn et al. (2014). Within that study, sequential extraction of natural reference soil showed, that Cu was mainly adsorbed to solid-phase organic matter or bound to poorly crystalline Fe(III) (oxyhydr)oxides. A smaller portion was also characterized as non-specifically adsorbed. In batch experiments of this study, mixing of soil and river water caused an immediate Cu mobilization in both CO₂ treatments and controls, which can be contributed to the release of weakly bound Cu. However, no order in mobilization rate according to temperature could be observed as it was for Mn, although the mobilization mechanism (competition with protons) should be similar for these cations. Copper is well known to form dissolved complexes with DOM (Blume et al., 2016), thus, the mixing of liquid and solid phase at the beginning of the experiment mobilized DOM and thereby might have also mobilized Cu through formation of dissolved Cu-DOM complexes. Unfortunately, we could not proof the existence of such complexes due to limited sample amount. At the moment, we also cannot exclude mobilization of particulate metallic Cu associated with microorganisms, as observed by Hofacker et al. (2015). Following this initial mobilization, Cu

concentrations in both controls and treatments stayed relatively constant, indicating that almost no Cu was incorporated into Fe(III) (oxyhydr)oxides or, alternatively, that Cu that was released by Fe(III) (oxyhydr)oxide dissolution could resorb immediately to other soil constituents. All these observations gave no hint on the net-immobilization of Cu that was observed in natural soil in Mehlhorn et al. (2014), but the fresh summer soil showed some interesting differences to all other batch experiments: following the initial concentration increase due to mixing of soil and water, the treatments showed a fast concentration decrease between 1 and 7 d followed by a slower decrease until the end of the experiment while the controls stayed relatively constant at the higher concentration level. Since the most obvious difference between fresh summer soil and spring soil is the higher organic matter content, resorption of Cu to solid organic matter could be a likely explanation for this decrease. Numerous studies have demonstrated the high affinity of Cu for organic matter (e.g. Brown et al., 2000; Kumpiene et al., 2007; McLaren and Crawford, 1973), however, the effect of CO₂ on this process has been unattended. The results presented in this study showed that under higher CO₂ partial pressure, Cu re-adsorption, most probably to solid organic matter, increased which supports the theory of a Cu net-immobilization in mofettes due to their higher organic matter content described in Mehlhorn et al. (2014). One possible explanation might be the formation of negatively charged Cu carbonate complexes (Cu(CO₃)₂²⁻) under high CO₂ partial pressures that can adsorb to the positively charged surfaces. However, geochemical modelling (PHREEQC Version 2.18.00) revealed negatively charged dissolved Cu carbonate complexes as minor species under the conditions given (data not shown). The formation of solid Cu carbonate minerals is also unlikely under the given acidic conditions. Another possible explanation already mentioned in Mehlhorn et al. (2014) is that Cu might have profited from the desorption of other cations (e.g. Mn) and attached to sorption sites previously covered by other elements. To completely clarify the process of Cu immobilization under CO₂ influence, further studies are required.

4.3. Implications for natural mofettes

The strong Fe mobilization observed in the CO₂ treatments of this study continued until the end of the experiments and no hint for approaching equilibrium could be seen. Similar to studies on Fe mobilization following a flooding event (e.g. Fiedler and Sommer, 2004; Meek et al., 1968; Ponnampereuma, 1972), the amount of Fe mobilized during the course of the experiment was small compared to the pool of total Fe available in the soil. It can thus be assumed that in case of a continuous CO₂ release into natural soil the Fe mobilization would have continued until Fe(III) (oxyhydr)oxide depletion. Assuming a continuous Fe mobilization with the rates calculated in Tables 3 and 4 and a total Fe(III) (oxyhydr)oxide content of approximately 11 mg g⁻¹ (Table 2), total depletion of Fe(III) (oxyhydr)oxides would have been reached after 280, 170, 46, and 16 years for C, RT, H1, and H3 treatments, respectively. Transferability of the exact rates determined in laboratory studies to the field is of course limited, because the calculation does not take into account any natural variations, like daily or seasonal changes in temperature or water regime. Nevertheless, they deliver a first estimate of minimum temperature-dependent time scales. Fe(III) (oxyhydr)oxides are almost completely absent in the center of the Czech mofette site, which is attributed to oxygen absence: Fe that is released during weathering cannot precipitate as (oxyhydr)oxides (Rennert et al., 2011, 2012). Since the mofettes in this area have formed at least decades or even centuries ago, this explanation is most likely, taking into account a continuous pedogenesis. However, data from our study give evidence that the formation of a new

CO₂ outgassing in a soil already rich in Fe(III) (oxyhydr)oxides can also lead to the microbially-triggered dissolution of Fe(III) (oxyhydr)oxides, despite the relatively high redox potential, which can be explained with the thermodynamic advantage of the proton consuming reduction process (Kirk et al., 2013). Toxic effects of high p(CO₂) on the microbial community were not observed in our study, as shown by constant MPNs. Beulig et al. (2016) also observed the ability of the microbial community from the reference soil to adapt to short-term (14 d) CO₂ exposure. However, CO₂ toxicity will probably be an issue considering long-term CO₂ influence on soils. Over longer time periods, a change in microbial community towards more CO₂ tolerant organisms and, after depletion of Fe(III) (oxyhydr)oxides, towards other functional groups (e.g. methanogens or acetogens, as detected in the center of the mofettes by Beulig et al. (2015)), could be expected.

The results of this study also confirmed the hypothesis from Mehlhorn et al. (2014) that the increased As mobility in natural mofettes is mainly caused by the absence of Fe(III) (oxyhydr)oxides, the most favored binding partner for As in the reference soil. They further provided some evidence for the hypothesis, that a net-immobilization of Cu occurs in the Czech mofettes, most probably due to increased resorption to solid organic matter under high p(CO₂). The results obtained for Mn did not necessarily help to answer the knowledge gaps on the Mn balance at the natural mofette site presented in Mehlhorn et al. (2014). There, both soil and liquid phase concentrations were decreased for Mn which contradicts the slight mobilization observed in this study. One important factor causing this discrepancy might be (reactive) transport of the liquid phase that cannot be taken into account in batch studies.

5. Conclusions

The results from this study increase our understanding regarding the kinetics and temperature dependency of soil processes following CO₂ intrusion into soil as it might occur during a CO₂ leakage from GCS sites or following the formation of a mofette. Within 1 h to 1 d the fast abiotic desorption of weakly bound cations due to competition with protons can be expected to cause a pore water concentration increase of some cationic elements. However, mobilization due to desorption was relatively small in the soil used in this study and resorption reactions could cause a complete re-immobilization over longer time periods. The risk for drinking water quality from a short-term CO₂ influence of <1 d on the considered soil is thus relatively low. Far more concerning are microbially-triggered mobilization processes, such as reductive dissolution of Fe(III) (oxyhydr)oxides in this study, since they tend to mobilize considerably larger amounts of certain elements (in this study especially Fe and As) than abiotic desorption. Higher temperatures as well as increased organic matter concentrations accelerated microbially-triggered Fe(III) (oxyhydr)oxide dissolution in our experiment. It can thus be assumed that biotically triggered mobilization processes will be enhanced in warm seasons and slowed down in cold seasons, while it will be the other way around for abiotic mobilization via desorption. This implies that GCS risk assessment should also take into account climatic factors. Our study also showed that pore water Fe concentrations could be a good additional short-term monitoring tool at sites with high Fe(III) (oxyhydr)oxide contents, where pH is no suitable monitoring parameter due to already low soil pH. However, distinguishing Fe mobilization caused by CO₂ intrusion from natural mobilization caused by changes in water regime in redoximorphic soils is difficult, but crucial for risk assessment, thus, the combined effects of water regime changes and temperature variations with CO₂ gas flow should be subject to further research.

Acknowledgements

We acknowledge financial support for a PhD stipend to Judith Mehlhorn from the German National Academic Foundation. We thank Kirsten Küsel (Aquatic Geomicrobiology, Friedrich Schiller University Jena) and Felix Beulig (Department of Bioscience, Aarhus University) for motivation to work on the mofettes, Stefan Will for help with ICP-MS analyses, Marcus Horn (Ecological Microbiology, University of Bayreuth) for help with MPN and interpretation of microbiological data, Ben Gilfedder and Silke Hammer (Hydrology, University of Bayreuth) for help with GC analysis and Martina Rohr (Hydrology, University of Bayreuth) for DOC analyses and help with nitrate analyses.

Appendix A. Supplementary data

Supplementary data related to this article can be found at <http://dx.doi.org/10.1016/j.apgeochem.2016.09.007>

References

- Bankwitz, P., Schneider, G., Kämpf, H., Bankwitz, E., 2003. Structural characteristics of epicentral areas in Central Europe: study case Cheb Basin (Czech Republic). *J. Geodyn.* 35, 5–32.
- Bauer, M., Blodau, C., 2006. Mobilization of arsenic by dissolved organic matter from iron oxides, soils and sediments. *Sci. Total Environ.* 354, 179–190.
- Bauer, M., Blodau, C., 2009. Arsenic distribution in the dissolved, colloidal and particulate size fraction of experimental solutions rich in dissolved organic matter and ferric iron. *Geochim. Cosmochim. Acta* 73, 529–542.
- Benz, M., Schink, B., Brune, A., 1998. Humic acid reduction by *Propionibacterium freudenreichii* and other fermenting bacteria. *Appl. Environ. Microbiol.* 64, 4507–4512.
- Berns, A., Philipp, H., Narres, H.-D., Burauel, P., Vereecken, H., Tappe, W., 2008. Effect of gamma-sterilization and autoclaving on soil organic matter structure as studied by solid state NMR, UV and fluorescence spectroscopy. *Eur. J. Soil Sci.* 59, 540–550.
- Beulig, F., Heuer, V.B., Akob, D.M., Viehweger, B., Elvert, M., Herrmann, M., Hinrichs, K.-U., Küsel, K., 2015. Carbon flow from volcanic CO₂ into soil microbial communities of a wetland mofette. *ISME J.* 9, 746–759.
- Beulig, F., Urich, T., Nowak, M., Trumbore, S.E., Gleixner, G., Gilfillan, G.D., Fjelland, K.E., Küsel, K., 2016. Altered carbon turnover processes and microbiomes in soils under long-term extremely high CO₂ exposure. *Nat. Microbiol.* 1, 15025.
- Blume, H.-P., Brümmer, G.W., Fleige, H., Horn, R., Kandeler, E., Kögel-Knabner, I., Kretzschmar, R., Stahr, K., Wilke, B.-M., 2016. Scheffer/Schachtschabel: Soil Science. Springer-Verlag, Berlin Heidelberg.
- Blume, H.-P., Felix-Henningsen, P., 2009. Reductosols: natural soils and technosols under reducing conditions without an aquatic moisture regime. *J. Plant Nutr. Soil Sci.* 172, 808–820.
- Borch, T., Kretzschmar, R., Kappler, A., Cappellen, P.V., Ginder-Vogel, M., Voegelin, A., Campbell, K., 2009. Biogeochemical redox processes and their impact on contaminant dynamics. *Environ. Sci. Technol.* 44, 15–23.
- Bräuer, K., Kämpf, H., Niedermann, S., Strauch, G., Weise, S.M., 2004. Evidence for a nitrogen flux directly derived from the European subcontinental mantle in the Western Eger Rift, central Europe. *Geochim. Cosmochim. Acta* 68, 4935–4947.
- Brechbühl, Y., Christl, I., Elzinga, E.J., Kretzschmar, R., 2012. Competitive sorption of carbonate and arsenic to hematite: combined ATR-FTIR and batch experiments. *J. Colloid Interface Sci.* 377, 313–321.
- Brown, P.A., Gill, S.A., Allen, S.J., 2000. Metal removal from wastewater using peat. *Water Res.* 34, 3907–3916.
- Chadwick, J., Jones, D., Thomas, M., Tatlock, G., Devenish, R., 1986. A Mössbauer study of ferrihydrite and aluminium substituted ferrihydrites. *J. Magn. Magn. Mater.* 61, 88–100.
- Chen, C., Kukkadapu, R., Sparks, D.L., 2015. Influence of coprecipitated organic matter on Fe²⁺_(aq)-catalyzed transformation of ferrihydrite: implications for carbon dynamics. *Environ. Sci. Technol.* 49, 10927–10936.
- CHMI, 2015. Czech Hydrometeorological Institute: Monthly Temperature and Precipitation Data for the Karlovy Vary Region retrieved from: <http://portal.chmi.cz>.
- Cornell, R.M., Schwertmann, U., 2003. In: *The Iron Oxides: Structure, Properties, Reactions, Occurrences and Uses*, second ed. John Wiley & Sons, Weinheim.
- Cullen, W.R., Reimer, K.J., 1989. Arsenic speciation in the environment. *Chem. Rev.* 89, 713–764.
- Dixit, S., Hering, J.G., 2003. Comparison of arsenic(V) and arsenic(III) sorption onto iron oxide minerals: implications for arsenic mobility. *Environ. Sci. Technol.* 37, 4182–4189.
- Fernández-Montiel, I., Sidrach-Cardona, R., Gabilondo, R., Pedescoll, A., Scheu, S., Bécares, E., 2016. Soil communities are affected by CO₂ belowground emissions at a natural vent in Spain. *Soil Biol. Biochem.* 97, 92–98.
- Fiedler, S., Sommer, M., 2004. Water and redox conditions in wetland soils - their influence on pedogenic oxides and morphology. *Soil Sci. Soc. Am. J.* 68, 326–335.
- Flechsig, C., Bussert, R., Rechner, J., Schütze, C., Kämpf, H., 2008. The Hartoušov mofette field in the Cheb Basin, western Eger Rift (Czech Republic): a comparative geoelectric, sedimentologic and soil gas study of a magmatic diffuse CO₂-degassing structure. *Z. Geol. Wiss.* 36, 177–193.
- Frerichs, J., Oppermann, B.L., Gwosdz, S., Möller, I., Herrmann, M., Krüger, M., 2013. Microbial community changes at a terrestrial volcanic CO₂ vent induced by soil acidification and anaerobic microhabitats within the soil column. *FEMS Microbiol. Ecol.* 84, 60–74.
- Goldberg, S., Johnston, C.T., 2001. Mechanisms of arsenic adsorption on amorphous oxides evaluated using macroscopic measurements, vibrational spectroscopy, and surface complexation modeling. *J. Colloid Interface Sci.* 234, 204–216.
- Harvey, O.R., Qafoku, N.P., Cantrell, K.J., Lee, G., Amonette, J.E., Brown, C.F., 2012. Geochemical implications of gas leakage associated with geologic CO₂ storage - a qualitative review. *Environ. Sci. Technol.* 47, 23–36.
- Harvey, O.R., Qafoku, N.P., Cantrell, K.J., Wilkins, M.J., Brown, C.F., 2016. Methanogenesis-induced pH-Eh shifts drives aqueous metal(loid) mobility in sulfide mineral systems under CO₂ enriched conditions. *Geochim. Cosmochim. Acta* 173, 232–245.
- Hofacker, A.F., Behrens, S., Voegelin, A., Kaegi, R., Lösekann-Behrens, T., Kappler, A., Kretzschmar, R., 2015. *Clostridium* species as metallic copper-forming bacteria in soil under reducing conditions. *Geomicrobiol. J.* 32, 130–139.
- IPCC, 2005. In: Metz, B., Davidson, O., De Coninck, H., Loos, M., Meyer, L. (Eds.), *IPCC Special Report on Carbon Dioxide Capture and Storage*, p. 442. Prepared by Working Group III of the Intergovernmental Panel on Climate Change.
- Jun, Y.-S., Giammar, D.E., Werth, C.J., 2012. Impacts of geochemical reactions on geologic carbon sequestration. *Environ. Sci. Technol.* 47, 3–8.
- Jun, Y.-S., Giammar, D.E., Werth, C.J., Dzombak, D.A., 2013. Environmental and geochemical aspects of geologic carbon sequestration: a special issue. *Environ. Sci. Technol.* 47, 1–2.
- Kämpf, H., Geissler, W.H., Bräuer, K., 2007. Combined gas-geochemical and receiver function studies of the Vogtland/NW Bohemia intraplate mantle degassing field, central Europe. In: Ritter, J.R.R., Christensen, U.R. (Eds.), *Mantle Plumes*. Springer, Berlin Heidelberg, pp. 127–158.
- Kappler, A., Benz, M., Schink, B., Brune, A., 2004. Electron shuttling via humic acids in microbial iron(III) reduction in a freshwater sediment. *FEMS Microbiol. Ecol.* 47, 85–92.
- Kharaka, Y.K., Cole, D.R., Hovorka, S.D., Gunter, W.D., Knauss, K.G., Freifeld, B.M., 2006. Gas-water-rock interactions in Frio Formation following CO₂ injection: implications for the storage of greenhouse gases in sedimentary basins. *Geology* 34, 577–580.
- Kharaka, Y.K., Thordsen, J.J., Kakouros, E., Ambats, G., Herkelrath, W.N., Beers, S.R., Birkholzer, J.T., Apps, J.A., Spycher, N.F., Zheng, L., Trautz, R.C., Rauch, H.W., Gullickson, K.S., 2010. Changes in the chemistry of shallow groundwater related to the 2008 injection of CO₂ at the ZERT field site, Bozeman, Montana. *Environ. Earth Sci.* 60, 273–284.
- Kirk, M.F., Santillan, E.F., Sanford, R.A., Altman, S.J., 2013. CO₂-induced shift in microbial activity affects carbon trapping and water quality in anoxic bioreactors. *Geochim. Cosmochim. Acta* 122, 198–208.
- Kirsch, K., Navarre-Sitchler, A.K., Wunsch, A., McCray, J.E., 2014. Metal release from sandstones under experimentally and numerically simulated CO₂ leakage conditions. *Environ. Sci. Technol.* 48, 1436–1442.
- Kumpiene, J., Lagerkvist, A., Maurice, C., 2007. Stabilization of Pb- and Cu-contaminated soil using coal fly ash and peat. *Environ. Pollut.* 145, 365–373.
- Lawter, A., Qafoku, N., Shao, H., Bacon, D., Brown, C., 2015. Evaluating impacts of CO₂ and CH₄ gas intrusion into an unconsolidated aquifer: fate of As and Cd. *Front. Environ. Sci.* 3, 49.
- Lawter, A., Qafoku, N.P., Wang, G., Shao, H., Brown, C.F., 2016. Evaluating impacts of CO₂ intrusion into an unconsolidated aquifer: I. Experimental data. *Int. J. Greenh. Gas Control* 44, 323–333.
- Lewicki, J.L., Birkholzer, J., Tsang, C.-F., 2007. Natural and industrial analogues for leakage of CO₂ from storage reservoirs: identification of features, events, and processes and lessons learned. *Environ. Geol.* 52, 457–467.
- Lions, J., Devau, N., De Lary, L., Dupraz, S., Parmentier, M., Gombert, P., Dictor, M.-C., 2014. Potential impacts of leakage from CO₂ geological storage on geochemical processes controlling fresh groundwater quality: a review. *Int. J. Greenh. Gas Control* 22, 165–175.
- Little, M.G., Jackson, R.B., 2010. Potential impacts of leakage from deep CO₂ sequestration on overlying freshwater aquifers. *Environ. Sci. Technol.* 44, 9225–9232.
- Lu, J., Partin, J.W., Hovorka, S.D., Wong, C., 2010. Potential risks to freshwater resources as a result of leakage from CO₂ geological storage: a batch-reaction experiment. *Environ. Earth Sci.* 60, 335–348.
- Maček, I., Videmšek, U., Kastelec, D., Stopar, D., Vodnik, D., 2009. Geological CO₂ affects microbial respiration rates in Stavesinci mofette soils. *Acta Biol. Slov.* 52, 41–48.
- McLaren, R.G., Crawford, D.V., 1973. Studies on soil copper II. The specific adsorption of copper by soils. *J. Soil Sci.* 24, 443–452.
- Meek, B.D., MacKenzie, A., Grass, L., 1968. Effects of organic matter, flooding time, and temperature on the dissolution of iron and manganese from soil in situ. *Soil Sci. Soc. Am. J.* 32, 634–638.
- Mehlhorn, J., Beulig, F., Küsel, K., Planer-Friedrich, B., 2014. Carbon dioxide triggered metal(loid) mobilisation in a mofette. *Chem. Geol.* 382, 54–66.

- Mehra, O., Jackson, M., 1960. Iron oxide removal from soils and clays by a dithionite-citrate system buffered with sodium bicarbonate. In: National Conference on Clays and Clays Minerals, pp. 317–327.
- Melton, E.D., Swanner, E.D., Behrens, S., Schmidt, C., Kappler, A., 2014. The interplay of microbially mediated and abiotic reactions in the biogeochemical Fe cycle. *Nat. Rev. Microbiol.* 12, 797–808.
- Mickler, P.J., Yang, C., Scanlon, B.R., Reedy, R., Lu, J., 2013. Potential impacts of CO₂ leakage on groundwater chemistry from laboratory batch experiments and field push-pull tests. *Environ. Sci. Technol.* 47, 10694–10702.
- Murad, E., 2010. Mössbauer spectroscopy of clays, soils and their mineral constituents. *Clay Miner.* 45, 413–430.
- Murad, E., Cashion, J., 2004. Mössbauer Spectroscopy of Environmental Materials and Their Industrial Utilization. Kluwer Academic Publishers, Dordrecht, the Netherlands.
- Nowak, M., Beulig, F., von Fischer, J., Muhr, J., Küsel, K., Trumbore, S.E., 2015. Autotrophic fixation of geogenic CO₂ by microorganisms contributes to soil organic matter formation and alters isotope signatures in a wetland mofette. *Biogeosciences* 12, 7169–7183.
- Oppermann, B.I., Michaelis, W., Blumenberg, M., Frerichs, J., Schulz, H.M., Schippers, A., Beaubien, S.E., Krueger, M., 2010. Soil microbial community changes as a result of long-term exposure to a natural CO₂ vent. *Geochim. Cosmochim. Acta* 74, 2697–2716.
- Pearce, J.M., 2006. What can we learn from natural analogues? In: Lombardi, S., Altunina, L.K., Beaubien, S.E. (Eds.), *Advances in the Geological Storage of Carbon Dioxide*. Springer, Netherlands, pp. 127–139.
- PIK, 2016. Potsdam Institute for Climate Impact Research: Ground Temperature - Mean Annual Variability retrieved from: <https://www.pik-potsdam.de/services/klima-wetter-potsdam/klimazeitreihen/bodentemperatur/>.
- Ponnamperuma, F.N., 1972. The chemistry of submerged soils. *Adv. Agron.* 24, 29–96.
- Porsch, K., Rijal, M.L., Borch, T., Troyer, L.D., Behrens, S., Wehland, F., Appel, E., Kappler, A., 2014. Impact of organic carbon and iron bioavailability on the magnetic susceptibility of soils. *Geochim. Cosmochim. Acta* 128, 44–57.
- R Development Core Team, 2008. R: a Language and Environment for Statistical Computing. R Foundation for Statistical Computing, Vienna, Austria.
- Rancourt, D., Ping, J., 1991. Voigt-based methods for arbitrary-shape static hyperfine parameter distributions in Mössbauer spectroscopy. *Nucl. Instrum. Methods Phys. Res. Sec. B* 58, 85–97.
- Raven, K.P., Jain, A., Loeppert, R.H., 1998. Arsenite and arsenate adsorption on ferrihydrite: kinetics, equilibrium, and adsorption envelopes. *Environ. Sci. Technol.* 32, 344–349.
- Redman, A.D., Macalady, D.L., Ahmann, D., 2002. Natural organic matter affects arsenic speciation and sorption onto hematite. *Environ. Sci. Technol.* 36, 2889–2896.
- Rennert, T., Eusterhues, K., Andrade, V.D., Totsche, K.U., 2012. Iron species in soils on a mofette site studied by Fe K-edge X-ray absorption near-edge spectroscopy. *Chem. Geol.* 332–333, 116–123.
- Rennert, T., Eusterhues, K., Pfanz, H., Totsche, K.U., 2011. Influence of geogenic CO₂ on mineral and organic soil constituents on a mofette site in the NW Czech Republic. *J. Soil Sci.* 62, 572–580.
- Rennert, T., Pfanz, H., 2015. Geogenic CO₂ affects stabilization of soil organic matter. *Eur. J. Soil Sci.* 66, 838–846.
- Ritter, K., Aiken, G.R., Ranville, J.F., Bauer, M., Macalady, D.L., 2006. Evidence for the aquatic binding of arsenate by natural organic matter-suspended Fe(III). *Environ. Sci. Technol.* 40, 5380–5387.
- Schütze, C., Sauer, U., Beyer, K., Lamert, H., Bräuer, K., Strauch, G., Flechsig, C., Kämpf, H., Dietrich, P., 2012. Natural analogues: a potential approach for developing reliable monitoring methods to understand subsurface CO₂ migration processes. *Environ. Earth Sci.* 67, 411–423.
- Schwertmann, U., 1964. Differenzierung der Eisenoxide des Bodens durch Extraktion mit Ammoniumoxalat-Lösung. *Z. Pflanzenernähr. Düngung Bodenkd.* 105, 194–202.
- Shao, H., Qafoku, N.P., Lawter, A.R., Bowden, M.E., Brown, C.F., 2015. Coupled geochemical impacts of leaking CO₂ and contaminants from subsurface storage reservoirs on groundwater quality. *Environ. Sci. Technol.* 49, 8202–8209.
- Sharma, P., Ofner, J., Kappler, A., 2010. Formation of binary and ternary colloids and dissolved complexes of organic matter, Fe and As. *Environ. Sci. Technol.* 44, 4479–4485.
- Sharma, P., Rolle, M., Kocar, B., Fendorf, S., Kappler, A., 2011. Influence of natural organic matter on As transport and retention. *Environ. Sci. Technol.* 45, 546–553.
- Šibanc, N., Dumbrell, A.J., Mandić-Mulec, I., Maček, I., 2014. Impacts of naturally elevated soil CO₂ concentrations on communities of soil archaea and bacteria. *Soil Biol. Biochem.* 68, 348–356.
- Smyth, R.C., Hovorka, S.D., Lu, J., Romanak, K.D., Partin, J.W., Wong, C., Yang, C., 2009. Assessing risk to fresh water resources from long term CO₂ injection – laboratory and field studies. *Energy Procedia* 1, 1957–1964.
- Stumm, W., Morgan, J.J., Drever, J.I., 1996. In: *Aquatic Chemistry: Chemical Equilibria and Rates in Natural Waters*, third ed. John Wiley & Sons, New York.
- Trevors, J., 1996. Sterilization and inhibition of microbial activity in soil. *J. Microbiol. Methods* 26, 53–59.
- Videmšek, U., Hagn, A., Suhadolc, M., Radl, V., Knicker, H., Schloter, M., Vodnik, D., 2009. Abundance and diversity of CO₂-fixing bacteria in grassland soils close to natural carbon dioxide springs. *Microb. Ecol.* 58, 1–9.
- Wang, S., Jaffe, P.R., 2004. Dissolution of a mineral phase in potable aquifers due to CO₂ releases from deep formations; effect of dissolution kinetics. *Energy Convers. Manage.* 45, 2833–2848.
- Zheng, L., Apps, J.A., Spycher, N., Birkholzer, J.T., Kharaka, Y.K., Thordsen, J., Beers, S.R., Herkelrath, W.N., Kakouros, E., Trautz, R.C., 2012. Geochemical modeling of changes in shallow groundwater chemistry observed during the MSU-ZERT CO₂ injection experiment. *Int. J. Greenh. Gas Control* 7, 202–217.
- Zheng, L., Apps, J.A., Zhang, Y., Xu, T., Birkholzer, J.T., 2009. On mobilization of lead and arsenic in groundwater in response to CO₂ leakage from deep geological storage. *Chem. Geol.* 268, 281–297.